

# Journal Pre-proof

Discovery of aryl-substituted indole and indoline derivatives as ROR $\gamma$ t agonists

Yan Zhu, Nannan Sun, Mingcheng Yu, Huimin Guo, Qiong Xie, Yonghui Wang



PII: S0223-5234(19)30723-8

DOI: <https://doi.org/10.1016/j.ejmech.2019.111589>

Reference: EJMECH 111589

To appear in: *European Journal of Medicinal Chemistry*

Received Date: 5 June 2019

Revised Date: 25 July 2019

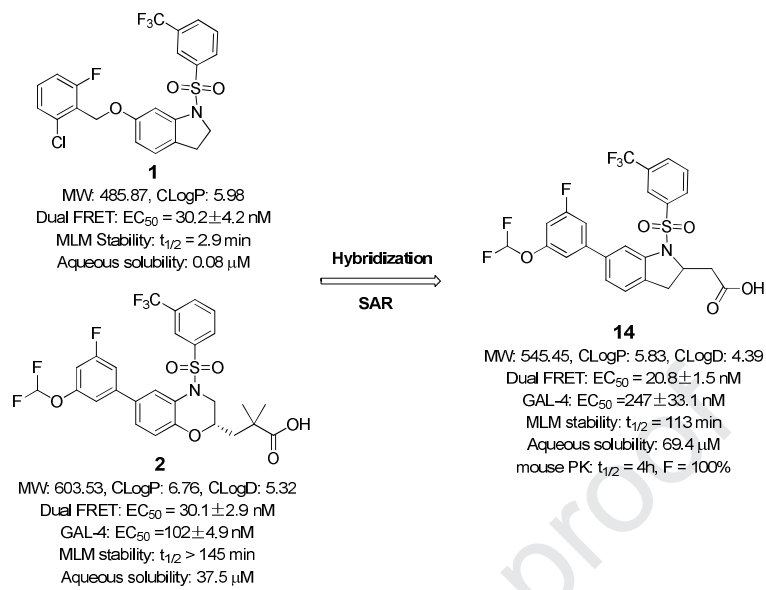
Accepted Date: 5 August 2019

Please cite this article as: Y. Zhu, N. Sun, M. Yu, H. Guo, Q. Xie, Y. Wang, Discovery of aryl-substituted indole and indoline derivatives as ROR $\gamma$ t agonists, *European Journal of Medicinal Chemistry* (2019), doi: <https://doi.org/10.1016/j.ejmech.2019.111589>.

This is a PDF file of an article that has undergone enhancements after acceptance, such as the addition of a cover page and metadata, and formatting for readability, but it is not yet the definitive version of record. This version will undergo additional copyediting, typesetting and review before it is published in its final form, but we are providing this version to give early visibility of the article. Please note that, during the production process, errors may be discovered which could affect the content, and all legal disclaimers that apply to the journal pertain.

© 2019 Published by Elsevier Masson SAS.

## Graphic Abstract



Discovery of Aryl-Substituted Indole and Indoline Derivatives as ROR $\gamma$ t Agonists

Yan Zhu<sup>#</sup>, Nannan Sun<sup>#</sup>, Mingcheng Yu, Huimin Guo, Qiong Xie\*, Yonghui Wang\*

*Department of Medicinal Chemistry, School of Pharmacy, Fudan University, 826 Zhangheng Road, Shanghai 201203, China*

<sup>#</sup> These authors contributed equally in this work.

\*Corresponding authors:

Tel & Fax: +86-21-51980122, *E-mail* address: qxie@fudan.edu.cn (Q. Xie);

Tel & Fax: +86-21-5198 0118, *E-mail* address: yonghuiwang@fudan.edu.cn (Y. Wang)

## Abstract:

A series of aryl-substituted indole and indoline derivatives were discovered as novel ROR $\gamma$ t agonists by a scaffold-based hybridization of the reported ROR $\gamma$ t agonists **1** and **2**. SAR studies on the core structures, the RHS hydrophilic side chains and the LHS hydrophobic aryl groups of a hybrid compound **3** led to the identification of potent ROR $\gamma$ t agonists with improved drug-like properties. Compound **14** represented a high potency lead with an EC<sub>50</sub> of 20.8  $\pm$  1.5 nM, the (*S*)-enantiomer (EC<sub>50</sub> = 16.1  $\pm$  4.5 nM) of which was 17 times more potent than the (*R*) counterpart (EC<sub>50</sub> = 286  $\pm$  30.4 nM) in ROR $\gamma$  dual FRET assay. The cell-based GAL4 reporter gene assay also suggested **14** as the most active compound which exhibited an EC<sub>50</sub> of 247  $\pm$  33.1 nM and a maximum activation percentage of 133%. Moreover, **14** showed high metabolic stability (*t*<sub>1/2</sub> = 113 mins) in mouse liver microsome and had improved aqueous solubility at pH 7.4 compared to the parent compounds. Furthermore, **14** was found to be orally bioavailable and demonstrated excellent *in vivo* pharmacokinetics in mice. Present studies indicate that **14** deserves further investigation in tumor animal models as a potential candidate of ROR $\gamma$ t agonist for cancer immunotherapy.

Keywords: indoles; indolines; ROR $\gamma$ t agonists; cancer immunotherapy; metabolic stability; aqueous solubility

## 1. Introduction

The T cell specific isoform of retinoic acid receptor-related orphan receptor gamma (ROR $\gamma$ ), known as ROR $\gamma$ t, is a nuclear receptor (NR) specifically expressed in thymocytes. ROR $\gamma$ t serves as a key transcription factor to drive the differentiation of CD4<sup>+</sup> cells into interleukin-17 (IL-17) producing T helper 17 (Th17) cells[1], which are implicated in the pathology of various inflammatory and autoimmune diseases[2, 3]. In addition to their major role in the field of autoimmune diseases[4, 5], ROR $\gamma$  antagonists were found to be effective in treating castration-resistant prostate cancer in a few articles[6, 7]. Recent studies have revealed the presence of Th17 cells in tumor microenvironment[8] and the active involvement of Th17 cells[9] and CD8<sup>+</sup> cytotoxic T (Tc17) cells[10] in protective tumor immunity by majorly producing IL17. Therefore, ROR $\gamma$ t has become a promising target with the potential of strengthening immune system to combat cancer. ROR $\gamma$ t agonists that promote the differentiation and activation of Th17 and Tc17 cells have shown promising therapeutic effects for cancer immunotherapy[11-13].

Starting from the discovery of ROR $\alpha/\gamma$  agonist SR1078[14], more and more small molecule agonists of ROR $\gamma$ t have been reported [13, 15-18] within researches on ROR $\gamma$ t inverse agonists. We previously reported the discovery and complex crystal structures of several *N*-aryl amide-based ROR $\gamma$ t agonists (Figure 1), such as tertiary amine (PDB: 4NIE)[19], thiazole amide (PDB: 4XT9)[20], thiazole ketone amide (PDB: 5YP5)[21] and biaryl amide (PDB: 5YP6)[21]. It was noticed that minor changes of ROR $\gamma$ t inverse agonists at the part interacting with activation function 2 (AF2) of the ligand binding domain (LBD) of ROR $\gamma$  could lead to functional switch from inhibition to activation[13, 17]. AF2 is a functional site of ROR $\gamma$ t-LBD around helix 11 (H11) and helix 12 (H12), which was stabilized by His479–Tyr502–Phe506  $\pi$ - $\pi$  cluster interactions.[13] ROR $\gamma$ t inverse agonists break the hydrogen bond between His479–Tyr502 and weaken the stabilization of AF2. Conversely, ROR $\gamma$ t agonists stabilize the AF2 conformation by forming hydrophobic interactions with Trp317, His479 and Tyr502, thus ROR $\gamma$ t are easier to recruit coactivator peptides.[17] The discovery of ROR $\gamma$ t agonists from ROR $\gamma$ t inverse agonists has been reported for some cases. However, reports about the structure-activity relationship (SAR) of ROR $\gamma$ t agonists remain limited.

Scripps reported the SAR study of a series of *N*-arylsulfonylindoline ROR $\gamma$ t agonists and found that an ether linker was preferred for ROR $\gamma$  agonism[22]. A representative compound **1** (Figures

2a and 3) exhibited good ROR $\gamma$  agonism activity ( $EC_{50} = 30.2 \pm 4.2$  nM, percent maximum activation (%Max) = 118%) in our ROR $\gamma$  dual fluorescence resonance energy transfer (dual FRET) assay. However, compounds of this series showed poor metabolic stability ( $t_{1/2} = 2.9$  mins for **1**) in mouse liver microsome (MLM) and had high lipophilicity (CLogP = 5.98 for **1**). Lycera's *N*-arylsulfonylbenzoxazine compound **2** (LYC-55716, Figures 2b and 3)[23] was the first drug candidate that entered phase 1/2 clinical trials for the treatment of solid tumors alone or in combination with programmed cell death protein 1 (PD-1) inhibitors[24]. Compound **2** was undoubtedly a potent ROR $\gamma$ t agonist ( $EC_{50} = 30.1 \pm 2.9$  nM, %Max = 152%) and showed high metabolic stability ( $t_{1/2} > 145$  mins) in MLM. However, compound **2** has a high molecular weight (MW) value of 603.53 and a high CLogP value of 6.76 which may need further optimization.

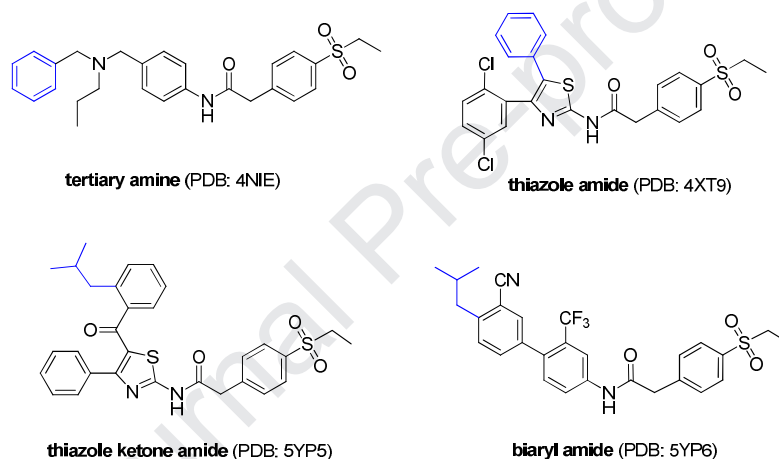


Figure 1. Reported *N*-aryl amide-based ROR $\gamma$ t agonists. (Parts of the agonist structures interacting with the AF2 domain of ROR $\gamma$  LBD were presented in blue.)

Docking modes of **1** and **2** in ROR $\gamma$ t LBD indicated that both left-hand side (LHS) moieties, namely the benzyl ether group and the phenyl group, occupied the same hydrophobic pocket near AF2 domain (Figure 2, the structural superimposition of compounds **1** and **2** in complex with ROR $\gamma$ t LBD is shown in Supplementary Figure S5). We hypothesized that replacing the 2-chloro-6-fluorobenzyl ether moiety of **1** with the 3-(difluoromethoxy)-5-fluorophenyl moiety of **2**, resulting in a hybrid compound **3** (Figure 3), could possibly maintain ROR $\gamma$ t activity based on the docking results of **3** (Figure 2 and Figure S6). Since there are two likely metabolic soft spots in compound **1**, namely the two benzylic positions [22], compound **3** with one of the metabolic spots the benzyl ether group removed might have improved its metabolic stability. Thus compound **3** was prepared and tested in ROR $\gamma$  dual FRET and MLM assays. To our delight, compound **3**

showed high ROR $\gamma$  agonism activity with an EC<sub>50</sub> of 50.6  $\pm$  4.6 nM and a maximum activation of 159%. However, the metabolic stability of **3** was a little better than that of **1** but remained low ( $t_{1/2}$  = 11.4 mins). Therefore, compound **3** needed further structural modifications on the indoline ring to improve the metabolic stability. In this paper, starting from the hybrid compound **3**, a series of aryl-substituted indole and indoline compounds were designed and synthesized by changing the indoline-like core structures, the right-hand side (RHS) 2- or 3-hydrophilic side chains and the LHS 6-aryl groups (Figure 3). Studies on the SAR, binding modes, *in vitro* metabolic stability, solubility and *in vivo* pharmacokinetic (PK) profiles of these compounds were further investigated to develop novel ROR $\gamma$ t agonists as potential therapeutic agents for cancer immunotherapy.

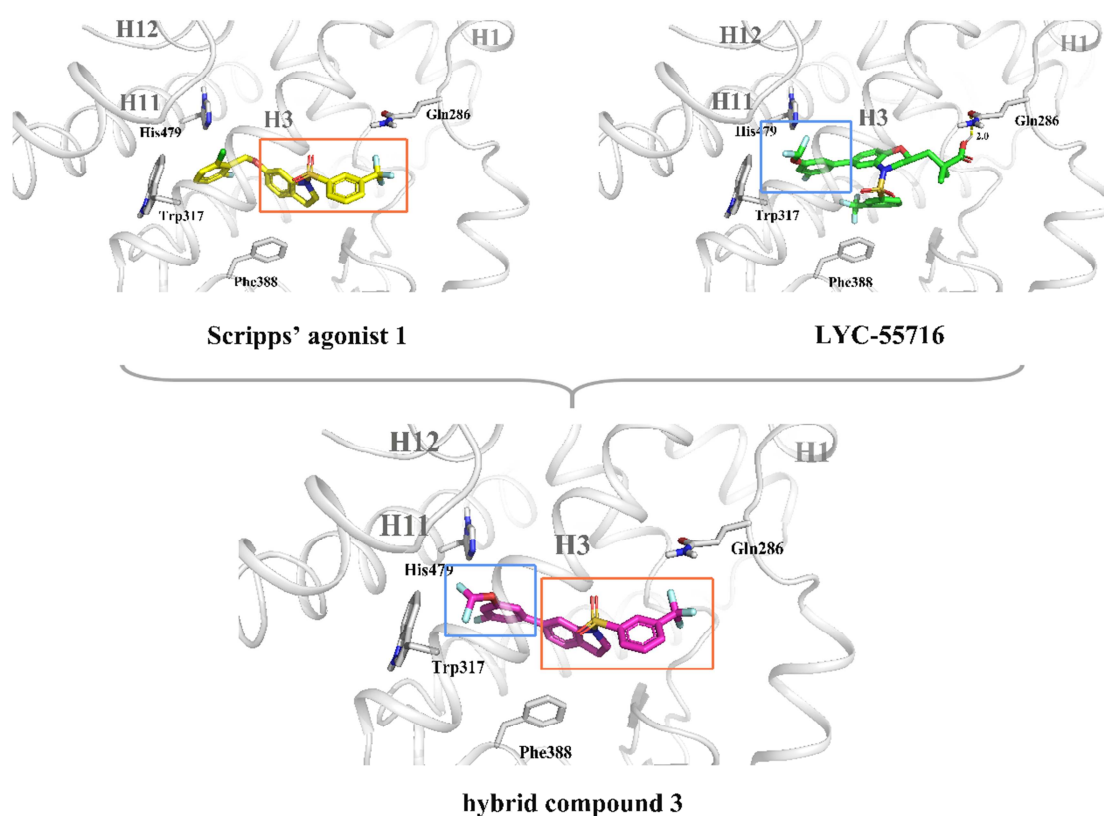


Figure 2. Docking poses of Scripps' agonist **1** (yellow stick), LYC-55716 **2** (green stick) and the hybrid compound **3** (magenta stick) in the binding pocket of ROR $\gamma$ t LBD (PDB ID: 4NIE).

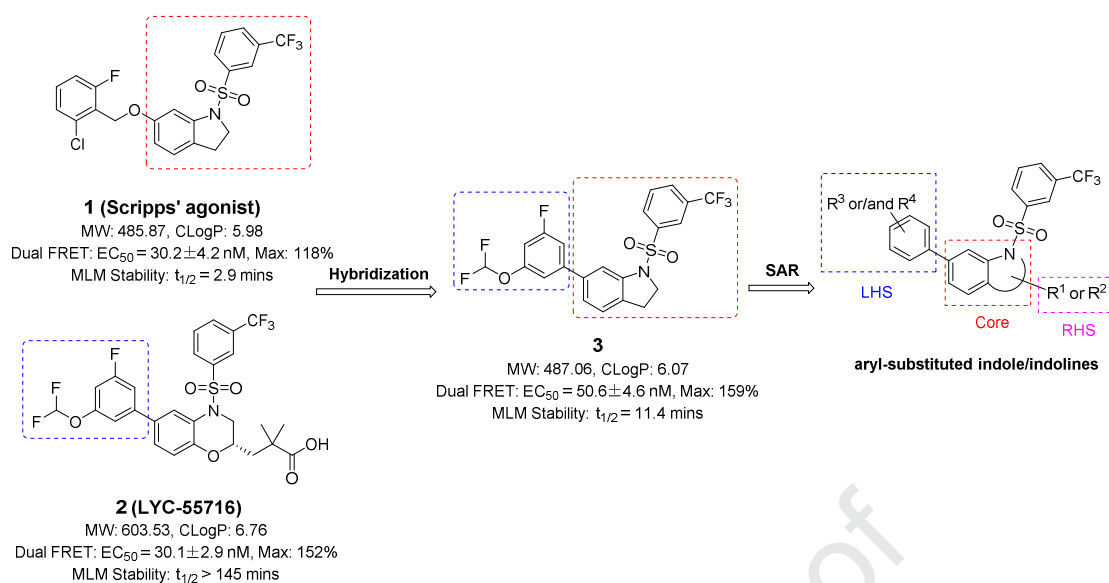


Figure 3. Hybridization strategy for the design of aryl-substituted indole/indolines as ROR $\gamma$ t agonists.

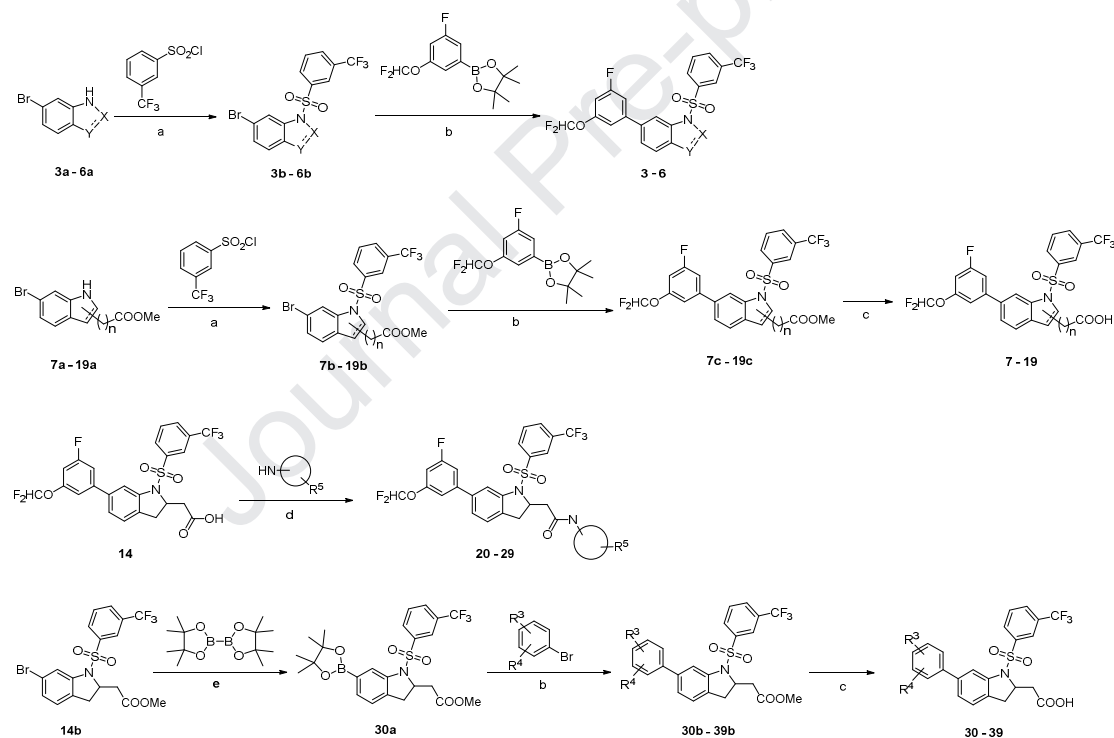
## 2. Results and Discussion

### 2.1 Compound design

We first optimized the core structures based on the principle of bioisosterism, by replacing the indoline of **3** with indole (**4**), indazole (**5**) and benzo[*d*]imidazole (**6**) moieties. After the optimal core structures identified, carboxylic acid side chains were attached to the 2- or 3- position of the preferred indole/indoline core structures via alkylene linkers of different length, leading to compounds **7–19**. According to the docking results of selected indole/indoline derivatives in ROR $\gamma$ t LBD, which indicated that the RHS parts participated in hydrogen-bonding interactions with hydrophilic residues, we designed compounds **20–29** with varied polar RHS groups substituted on 2-position of the indoline scaffold. In contrast, the LHS parts were involved in hydrophobic contacts with AF2. Therefore, compounds **30–39** with different lipophilic substituents on the LHS aryl group were designed and synthesized (Figure 4).



3-(difluoromethoxy)-5-fluorophenyl boronic acid pinacol ester yielded the corresponding compounds **3–6**. Intermediates **7c–19c** were obtained by the same procedures of sulfonylation and Suzuki coupling reaction from **7a–19a**, the synthesis of which was presented in Supporting Information. Final hydrolysis of **7c–19c** in THF by LiOH gave the carboxylic acid compounds **7–19**. Amide condensation of compound **14** with a set of cyclic secondary amines under the condition of HATU and DIEA afforded the targeted compounds **20–29**. A palladium-catalyzed Suzuki coupling reaction using substituted bromobenzene and **30a**, which was prepared from **14b**, gave intermediates **30b–39b**. Subsequent hydrolysis of **30b–39b** by LiOH yielded the desired compounds **30–39**. Enantiomers (*S*)-**14** and (*R*)-**14** were obtained by chiral HPLC separation of the racemate compound **14**. Besides, the absolute configurations were determined according to the optical rotation values of (*S*)-**14** and (*R*)-**14** compared with that of compound **2**.



Scheme 1. General synthetic procedures for the aryl-substituted indole/indoline compounds.

Reagents and conditions: a) DMAP, DIEA, DCM, rt, 12 h; b) Pd<sub>2</sub>(dba)<sub>3</sub>, X-Phos, K<sub>2</sub>CO<sub>3</sub>, 1,4-Dioxane, N<sub>2</sub>, 100 °C, 12 h; c) LiOH, THF, rt, 5 h; d) HATU, DIEA, DCM, 30 °C, 3–12 h; e) Pd(dppf)Cl<sub>2</sub>, KOAc, 1,4-Dioxane, N<sub>2</sub>, 100 °C, 12 h.

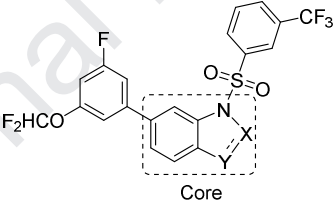
### 2.3 Structure-activity relationship

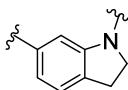
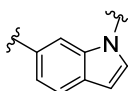
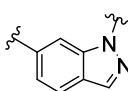
The synthesized compounds were evaluated in ROR<sub>γ</sub> dual FRET assay according to the basal

level activity changes, which is suitable for the activity and function assessment of both agonists and inverse agonists.[19] Compounds in each set having good ROR $\gamma$ t agonism activities were subjected to metabolic stability assay in MLM and cell-based GAL4 luciferase reporter gene assay.

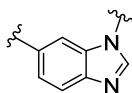
Initially, a set of compounds with different 5-, 6-membered bicyclic cores (**3-6**) were designed, synthesized and evaluated in the ROR $\gamma$  dual FRET assay (Table 1). With indole replacing the indoline in **3**, compound **4** showed a two-fold reduction in ROR $\gamma$ t activity ( $EC_{50} = 99.4 \pm 44.7$  nM) and a slight drop in efficacy (%Max = 125%) relative to **3**. On the other hand, the indole compound **4** showed improved metabolic stability in MLM, with a  $t_{1/2}$  of 39.1 mins, 3-times longer than that of **3**. When the core structure was replaced by indazole (**5**) or benzo[*d*]imidazole (**6**), both ROR $\gamma$ t potency and efficacy reduced. In view of the ROR $\gamma$ t activity and metabolic stability, we chose indole in **4** and indoline in **3** as preferred core structures for the following RHS optimization.

Table 1. SAR of core structures



Compd	Core	CLogP <sup>a</sup>	ROR $\gamma$ dual FRET		MLM Stability <sup>d</sup>
			$EC_{50}$ (nM) <sup>b</sup>	%Max <sup>c</sup>	$t_{1/2}$ (mins)
<b>1</b> (Scripps' agonist)		5.98	<b>30.2 ± 4.2</b>	118	2.9
<b>2</b> (LYC-55716)		6.76	<b>30.1 ± 2.9</b>	152	>145
<b>3</b>		6.07	<b>50.6 ± 4.6</b>	159	11.4
<b>4</b>		6.95	<b>99.4 ± 44.7</b>	125	39.1
<b>5</b>		6.30	<b>205 ± 35</b>	75	- <sup>e</sup>

6



6.17

122 ± 101

75

-<sup>e</sup>

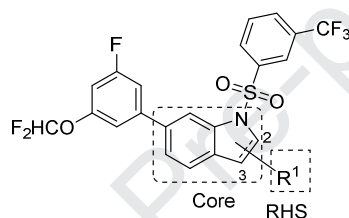
<sup>a</sup> Calculated by Discovery Studio 3.0. <sup>b</sup> EC<sub>50</sub> value was expressed as Mean ± SD, n=2. <sup>c</sup> Percent maximum activation. <sup>d</sup> Mouse liver microsomes stability test. <sup>e</sup> “-” means not determined.

After identifying the preferred core structures, we explored SAR of the RHS moiety of **4** and **3**. Introduction of a carboxylic acid tether to the selected indole/indoline cores was expected to maintain RORγt activity and make improvement in metabolic stability. Compounds **7-19** with carboxylic acid tethered by alkylene chains of different length to the 2- or 3- position of indole/indoline were designed and synthesized. Results of their RORγt activity, metabolic stability and cell-based gene transcription activity were summarized in Table 2. Indole-2-carboxylic acid analogue **7** showed essentially the same RORγt potency and efficacy as **4** while the 2-acetic acid derivative **8** exhibited a lower RORγt activity. Elongating the linker by adding ethylene resulted in 2-propionic acid compound **9**, which was 3-fold more active than **4** in activating RORγt. Further elongation of the linker from ethylene to propylene (**10**) slightly lowered the RORγt activity relative to **9**. Switching the carboxylic acid tethers to 3-position (**11-13**) reduced the RORγt potency and efficacy comparing with their 2-position counterparts (**8-10**). Among the indole series, **9** stood out with an EC<sub>50</sub> of 25.5 ± 11.6 nM and a maximum activation of 124%, and was then subjected to *in vitro* metabolic stability assay which indicated a high stability of **9** in MLM (t<sub>1/2</sub> > 145 mins) like Lycera’s compound **2**. However, in cell-based reporter gene assay, **9** only displayed activity at micromolar level with an EC<sub>50</sub> of 1710 ± 396 nM, 16-fold less potent than **2** (EC<sub>50</sub> = 102 ± 4.9 nM). This could be explained by the increased lipophilicity (CLogP and CLogD) of **9** which may affect cell permeability.

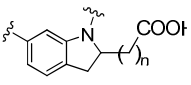
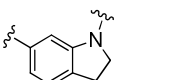
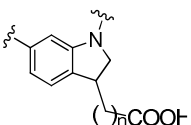
All carboxylic acid-tethered indoline compounds (**14-19**) showed high RORγt potency with EC<sub>50</sub>s ranging from 14.6 nM to 31.3 nM, no matter tethered at 2- or 3- position. As for the maximum activation response, 2-substituted indolines (%Max ~ 120%) outperformed 3-substituted indolines (%Max ~ 100%). Compounds **14** and **17** with a side chain of acetic acid tethered at the 2- and the 3- position, respectively, exhibited the highest RORγt potency and efficacy among each subset of the indoline series. In the next MLM stability test, 2-substituted indolines (t<sub>1/2</sub> > 60 mins) were obviously more stable than 3-substituted indolines (t<sub>1/2</sub> < 50 mins). It seems that metabolic

stability increases with an order of the linker length ( $n$ ) of  $2 < 3 < 1$ , so does the cell-based activity. Taking both the cell-based ROR $\gamma$ t activity and metabolic stability into account, compound **14** ( $EC_{50} = 247 \pm 33.1$  nM, %Max = 133%,  $t_{1/2} = 113$  mins) stood out among the indoline series. We separated two enantiomers of **14** by chiral HPLC, and (*S*)-enantiomer ( $EC_{50} = 16.1 \pm 4.5$  nM) showed 17 times higher potency than (*R*)-enantiomer ( $EC_{50} = 286 \pm 30.4$  nM) in ROR $\gamma$ t dual FRET assay. The activity of (*S*)-**14** on GAL4 luciferase reporter gene assay ( $EC_{50} = 201 \pm 48.9$  nM, %Max = 144%) was correlated with the dual FRET result, which both suggested (*S*)-**14** as the optimal enantiomer.

Table 2. SAR of RHS moiety



Compd	Core+RHS	n	CLogP/ CLogD <sup>a</sup>	ROR $\gamma$ dual FRET		MLM Stability <sup>d</sup> $t_{1/2}$ (mins)	GAL4 <sup>e</sup>	
				$EC_{50}$ (nM) <sup>b</sup>	%Max <sup>c</sup>		$EC_{50}$ (nM) <sup>b</sup>	$E_{max}$ (%)
<b>2</b>			6.76/5.32	<b>30.1 <math>\pm</math> 2.9</b>	152	>145	<b>102 <math>\pm</math> 4.9</b>	141
<b>7</b>		0	6.87/5.41	<b>74.3 <math>\pm</math> 21.1</b>	128	- <sup>f</sup>	- <sup>f</sup>	- <sup>f</sup>
<b>8</b>		1	6.91/5.46	<b>125 <math>\pm</math> 4.4</b>	66	-	-	-
<b>9</b>		2	6.94/5.47	<b>25.5 <math>\pm</math> 11.6</b>	124	>145	<b>1710 <math>\pm</math> 396</b>	74
<b>10</b>		3	7.40/5.98	<b>45.3 <math>\pm</math> 19.9</b>	95	-	-	-
<b>11</b>		1	6.62/5.17	<b>133 <math>\pm</math> 17.8</b>	62	-	-	-
<b>12</b>		2	7.07/5.61	<b>43.6 <math>\pm</math> 29.7</b>	71	-	-	-
<b>13</b>		3	7.53/6.07	<b>93.8 <math>\pm</math> 22.6</b>	74	-	-	-

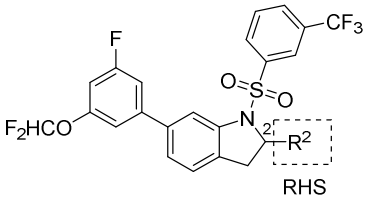
<b>14</b>		1	5.83/4.39	20.8 ± 1.5	127	113	247 ± 33.1	133
<b>(S)-14</b>		1	5.83/4.39	16.1 ± 4.5	124	-	201 ± 48.9	144
<b>(R)-14</b>		1	5.83/4.39	286 ± 30.4	93	-	-	-
<b>15</b>		2	6.15/4.70	31.3 ± 9.1	123	60.9	2320 ± 1560	172
<b>16</b>		3	6.61/5.18	25.2 ± 3.4	117	93.3	422 ± 43.2	146
<b>17</b>		1	5.57/5.02	21.8 ± 1.2	109	45.6	-	-
<b>18</b>		2	6.02/4.57	14.6 ± 2.2	97	24.5	-	-
<b>19</b>		3	6.48/5.29	26.2 ± 11.6	95	34.2	-	-

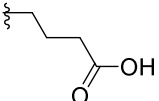
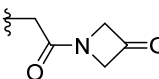
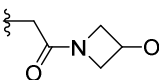
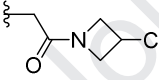
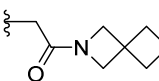
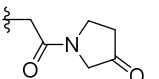
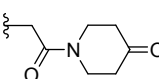
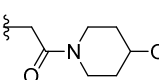
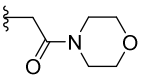
<sup>a</sup> Calculated by Discovery Studio 3.0. <sup>b</sup>EC<sub>50</sub> value was expressed as Mean ± SD, n=2. <sup>c</sup> Percent maximum activation. <sup>d</sup> Mouse liver microsome stability test. <sup>e</sup> GAL4 reporter gene assay. <sup>f</sup> “-” means not determined.

Compound **16** showed good cell-based ROR $\gamma$ t activity (EC<sub>50</sub> = 422 ± 43.2 nM, %Max = 146%) and metabolic stability (t<sub>1/2</sub> = 93.3 mins) as well, but it had a high CLogP of 6.61. We tried to modify the RHS butyric acid of **16** with different amide-connected polar groups, including ketones, alcohols, carboxylic acids, ethers and sulfone. All designed compounds (**20-29**) had lower CLogP values compared to **16** and showed equivalent or higher maximum activation response in ROR $\gamma$ t dual FRET assay (Table 3). As different groups substituted on R<sup>2</sup>, their ROR $\gamma$ t activation potencies increased by the order of alcohol (**21**) < ether (**27**) < ketone (**20, 24, 25**) < carboxylic acid (**22, 28**) < sulfone (**29**). The more unique were **23** with a 2-oxa-6-azaspiro[3.3]heptanyl group and **26** with a 4-hydroxypiperidinyl group, which represented more active compounds within the ether and alcohol series, respectively, and were subjected to metabolic stability and GAL4 reporter gene assays along with carboxylic acids (**22, 28**) and sulfone (**29**). Results were summarized in Table 3. The cell-based activities of two carboxylic acids (**22, 28**) and alcohol (**26**) dropped dramatically with EC<sub>50</sub>s of 4 to 6  $\mu$ M, although the metabolic stability of carboxylic acids was acceptable (t<sub>1/2</sub> 30~66 mins) while the alcohol metabolized very quickly. To our surprise, **23** was fairly unstable in MLM and was destroyed within one minute (t<sub>1/2</sub> < 1 min), although it showed submicromolar

ROR $\gamma$ t activity in GAL4 reporter gene assay ( $EC_{50} = 752 \pm 100$  nM). The most potent sulfone compound **29** was 1.3 times more active than **16** in GAL4 reporter gene assay, displaying an  $EC_{50}$  of  $322 \pm 51.4$  nM. Unfortunately, the half-life of **29** in MLM was as low as 2 minutes, which prevent it from further development.

Table 3. SAR of the R<sup>2</sup> of RHS moiety



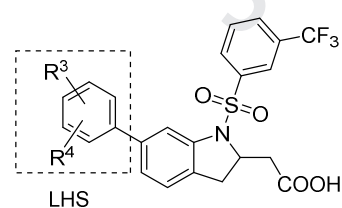
Compd	RHS (R <sup>2</sup> )	CLogP <sup>a</sup>	ROR $\gamma$ dual FRET		MLM Stability <sup>d</sup> t <sub>1/2</sub> (mins)	GAL4 <sup>e</sup>	
			EC <sub>50</sub> (nM) <sup>b</sup>	%Max <sup>c</sup>		EC <sub>50</sub> (nM) <sup>b</sup>	E <sub>max</sub> (%)
<b>16</b>		6.61	25.2 ±	117	93.3	422 ±	146
			3.4			43.2	
<b>20</b>		4.88	78.8 ±	130	_f	_f	_f
			13.7			_f	
<b>21</b>		4.92	244 ±	141	-	-	-
			17.4			-	
<b>22</b>		5.07	49.3 ±	138	65.9	4050 ±	100
			21.6			459	
<b>23</b>		4.93	47.9 ±	128	0.7	752 ±	104
			3.0			100	
<b>24</b>		5.13	52.3 ±	136	-	-	-
			18.5			-	
<b>25</b>		5.38	80.4 ±	136	-	-	-
			1.0			-	
<b>26</b>		5.05	106 ±	127	0.7	6040 ±	100
			9.7			1010	
<b>27</b>		5.30	209 ±	128	-	-	-

			90.6				
<b>28</b>		5.71	57.1 ± 6.8	116	30.1	5440 ± 3360	178
<b>29</b>		5.03	43.4 ± 19.9	126	2.0	322 ± 51.4	104

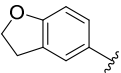
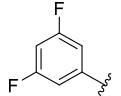
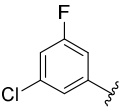
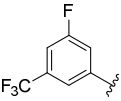
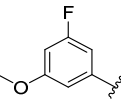
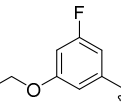
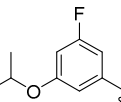
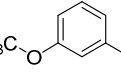
<sup>a</sup> Calculated by Discovery Studio 3.0. <sup>b</sup>EC<sub>50</sub> value was expressed as Mean ± SD, n=2. <sup>c</sup> Percent maximum activation. <sup>d</sup> Mouse liver microsome stability test. <sup>e</sup>GAL4 reporter gene assay. <sup>f</sup>“-” means not determined.

Based on the above SAR studies on core structure and RHS moiety, **14** was selected as the template to make LHS modifications. We first made cyclization at the 3- and 4- position of the phenyl group, yielding benzo[*d*][1,3]dioxole and 2,3-dihydrobenzofuran derivatives (**30-32**), which were less potent than **14** in RORγt dual FRET assay (Table 4). Changes were then made on the 3-difluoromethoxyl group by halogens (**33, 34**), trifluoromethyl group (**35**) and alkoxy groups (**36-39**), but no activity enhancement was observed as shown in Table 4. Introduction of an isopropoxy group (**38**) caused the greatest activity reduction in this series probably due to increased size of the substituent, which may interfere with interactions between the LHS of **38** and the AF2 of RORγt LBD.

Table 4. SAR of LHS moiety



Compd	LHS	CLogP/ CLogD <sup>a</sup>	RORγ dual FRET	
			EC <sub>50</sub> (nM) <sup>b</sup>	%Max <sup>c</sup>
<b>14</b>		5.83/4.39	20.8 ± 1.5	127
<b>30</b>		6.62/5.18	42.6 ± 6.0	90
<b>31</b>		4.59/3.15	87.4 ± 20.5	77

32		4.88/3.44	56.8 ± 21.0	40
33		5.23/3.79	25.7 ± 4.8	101
34		5.69/4.25	42.0 ± 4.8	98
35		5.97/4.53	41.3 ± 5.2	115
36		5.01/3.57	39.3 ± 1.1	88
37		5.36/3.92	32.9 ± 10.9	96
38		5.73/4.30	124 ± 63.8	105
39		6.94/5.50	31.1 ± 5.7	95

<sup>a</sup> Calculated by Discovery Studio 3.0. <sup>b</sup>EC<sub>50</sub> value was expressed as Mean ± SD, n=2. <sup>c</sup> Percent maximum activation.

## 2.4 Binding mode study

The binding mode of (*S*)-**14** in ROR $\gamma$ t LBD was revealed by docking study (Figure 5). In the most possible binding mode, the 3-(difluoromethoxy)-5-fluorophenyl moiety in the LHS of the indoline core locates in the functional site around H11 and H12, forming  $\pi$ - $\pi$  stacking interactions with His479 and Trp317 and stabilizing the AF2 domain. This moiety occupies in almost the same place as that in the initial compound **2** (LYC-55716), which is believed to be the functional group for our compounds possessing the ROR $\gamma$ t agonist activity (shown as Figure 5b). In the RHS, the acetic acid group formed hydrogen bonds with the main chain of His323. Besides, the 3-trifluoromethyl substituted phenylsulfony moiety is in a hydrophobic cavity, forming  $\pi$ - $\pi$  stacking interactions with Phe377 and providing preferred intermolecular interactions with

surrounding hydrophobic residues in the hydrophobic site near Phe377 and Phe378.

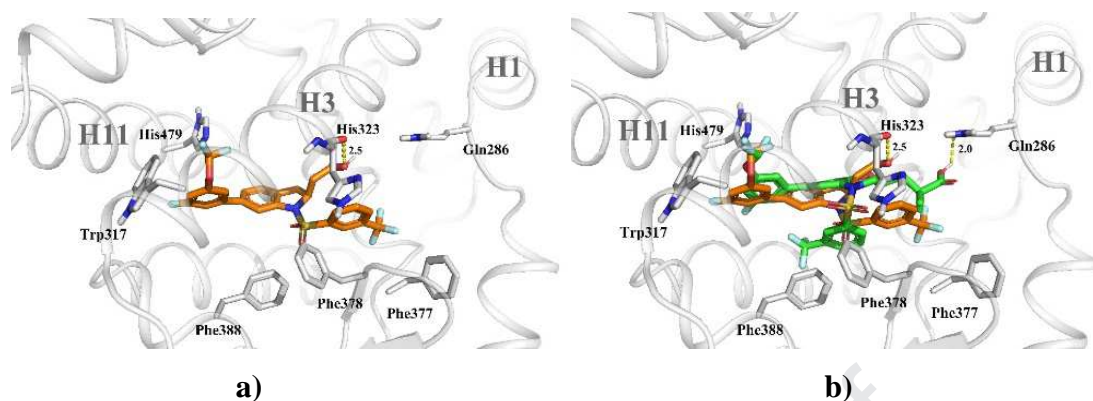


Figure 5. a) Zoomed-in view of (*S*)-**14** in the binding pocket of ROR $\gamma$ t LBD. (PDB ID: 4NIE, (*S*)-**14** is in orange stick); b) Structural superimposition of **2** (green stick) with (*S*)-**14** (orange stick) in ROR $\gamma$ t LBD.

## 2.5 Drug-like properties and PK study

The solubility of **1**, **2**, **3** and **14** in aqueous solution at the condition of pH 7.4 was subsequently evaluated. Results were shown in Table 5. Compounds **1** and **3** showed relatively poor solubility (< 2  $\mu$ M) because they have high lipophilicity and are lack of ionic or ionizable group. The aqueous solubility of compounds **2** ( $S = 37.5 \mu$ M) and **14** ( $S = 69.4 \mu$ M) dramatically increased due to the introduction of ionic carboxylic acid groups. Compound **14** was 2 times more soluble than compound **2**, which could be explained by the decreased MW and CLogP (5.83)/CLogD (4.39) values of **14**. The PK of **14** was investigated in mice following intravenous (IV, 1 mg/kg) and oral (PO, 5 mg/kg) administration. Compound **14** showed low *in vivo* clearance (CL = 0.573 L/h/kg), a moderate half-life of 4 h and a high oral bioavailability of 100% (see Table S4 and Figure S7). Overall, compound **14** demonstrated excellent *in vivo* pharmacokinetics in mice consistent with its *in vitro* properties (aqueous solubility and metabolic stability).

Table 5. Summary of the drug-like properties of selected compounds **1-3**, **14**.

Compds	MW	CLogP/CLogD <sup>a</sup>	Solubility <sup>b</sup> ( $\mu$ M)	MLM Stability <sup>c</sup> $t_{1/2}$ (mins)	CL <sub>int(mic)</sub> <sup>d</sup> ( $\mu$ L/min/mg)
<b>1</b> (Scripps)	485.87	5.98/5.98	0.08	2.9	482

agonist)					
<b>2</b> (LYC-55716)	603.53	6.76/5.32	37.5	>145	< 9.6
<b>3</b>	487.06	6.07/6.07	1.48	11.4	121
<b>14</b>	545.45	5.83/4.39	69.4	113	12.3

<sup>a</sup> Calculated by Discovery Studio 3.0. <sup>b</sup> Kinetic aqueous solubility at pH 7.46. <sup>c</sup> Mouse liver microsome stability test. <sup>d</sup> Intrinsic clearance per mg microsome protein per mL.

### 3. Conclusions

In conclusion, we have discovered a series of aryl-substituted indole and indoline derivatives as novel ROR $\gamma$ t agonists by a scaffold-based hybridization strategy. SAR studies on the core structures, RHS hydrophilic side chains and LHS hydrophobic aryl groups of the hybrid compound **3** led to the identification of potent ROR $\gamma$ t agonists with improved drug-like properties. Compound **14** was found to have good ROR $\gamma$ t activities in both dual FRET and GAL4 reporter gene assays. Compound **14** showed high metabolic stability in MLM and had improved aqueous solubility (2-fold relative to **2**) at pH 7.4. Furthermore, **14** demonstrated excellent oral bioavailability and *in vivo* PK profile in mice. Present studies suggest **14** as a potential ROR $\gamma$ t agonist candidate which deserves further investigation in tumor animal models for cancer immunotherapy.

### 4. Experimental

#### 4.1 Materials and Methods

All commercially available reagents were used without further purification unless otherwise stated. The reactions were monitored by thin-layer chromatography (TLC) analysis. Silica gel (200-300 mesh) was used for column chromatography. The purity of all test compounds was assessed by HPLC and area % purity was measured at 254 nm. The HPLC analyses were performed using a Agilent 1260 instrument. Elution was done with a gradient of 5–90% solvent B (acetonitrile with 0.1% TFA) in solvent A (water with 0.1% TFA) through an Agilent HC-C18(2) (4.6 mm  $\times$  150 mm, 5  $\mu$ m) column at 3.0 mL/min. High-resolution MS (HRMS) was analyzed by a TOF analyzer. The ion source is electrospray ionization (ESI). <sup>1</sup>H NMR spectra were recorded at 400 MHz and

$^{13}\text{C}$  NMR spectra were recorded at 600 MHz. Chemical shifts in  $^1\text{H}$  NMR spectra are reported in parts per million (ppm) on the  $\delta$  scale from an internal standard of  $\text{CDCl}_3$  (7.26 ppm). Data are reported as follows: chemical shift ( $\delta$  ppm), multiplicity (s = singlet, d = doublet, t = triplet, q = quartet, m = multiplet, br = broad), coupling constant in hertz (Hz), and integration. Chemical shifts of  $^{13}\text{C}$  NMR spectra are reported in ppm from the central peak of  $\text{CDCl}_3$  (77.0 ppm) on the  $\delta$  scale.

## 4.2 Chemical Synthesis

### 4.2.1 The synthesis of compounds 1–2

Compounds **1** and **2** were synthesized following the published procedures[19, 22], and were characterized by  $^1\text{H}$  NMR,  $^{13}\text{C}$  NMR and MS.

4.2.1.1 6-((2-Chloro-6-fluorobenzyl)oxy)-1-((3-(trifluoromethyl)phenyl)sulfonyl)indoline (**1**). Yield: 81%, white solid, purity: 98%.  $^1\text{H}$  NMR (400 MHz,  $\text{DMSO-}d_6$ )  $\delta$  (ppm) 8.15 (d,  $J = 7.5$  Hz, 1H), 8.09 (d,  $J = 7.1$  Hz, 1H), 8.02 (s, 1H), 7.84 (t,  $J = 6.6$  Hz, 1H), 7.51 (dd,  $J = 14.4, 7.8$  Hz, 1H), 7.43 (d,  $J = 7.8$  Hz, 1H), 7.33 (t,  $J = 8.2$  Hz, 1H), 7.11 – 7.07 (m, 2H), 6.71 (d,  $J = 8.1$  Hz, 1H), 5.15 (s, 2H), 3.99 (t,  $J = 6.7$  Hz, 2H), 2.82 (t,  $J = 7.1$  Hz, 2H);  $^{13}\text{C}$  NMR (150 MHz,  $\text{DMSO-}d_6$ )  $\delta$  (ppm) 162.1, 160.4, 158.0, 141.8, 137.2, 135.3 (d,  $J = 4.8$  Hz), 131.6 (d,  $J = 9.8$  Hz), 130.4 (d,  $J = 2.5$  Hz), 129.9 (q,  $J = 32.8$  Hz), 125.9, 125.6, 124.8, 123.9, 123.3 (d,  $J = 3.4$  Hz), 122.1, 121.8 (d,  $J = 17.7$  Hz), 114.6 (d,  $J = 22.5$  Hz), 110.5, 101.7, 61.4 (d,  $J = 3.0$  Hz), 50.8, 26.4; MS (ESI)  $m/z$  486.1  $[\text{M} + \text{H}]^+$ .

### 4.2.1.2

(*S*)-3-(6-(3-(Difluoromethoxy)-5-fluorophenyl)-4-((3-(trifluoromethyl)phenyl)sulfonyl)-3,4-dihydro-2H-benzo[*b*][1,4]oxazin-2-yl)-2,2-dimethylpropanoic acid (**2**). Yield: 67%, white solid, purity: 95%.  $[\alpha]_D^{23} +147^\circ$  ( $c = 0.2$ ,  $\text{CH}_2\text{Cl}_2$ ).  $^1\text{H}$  NMR (400 MHz,  $\text{DMSO-}d_6$ )  $\delta$  (ppm) 12.28 (s, 1H), 8.14 (d,  $J = 7.7$  Hz, 1H), 7.95 (dd,  $J = 8.2, 6.4$  Hz, 3H), 7.85 (t,  $J = 7.9$  Hz, 1H), 7.60 – 7.42 (m, 2H), 7.34 (d,  $J = 9.7$  Hz, 1H), 7.24 (s, 1H), 7.13 (d,  $J = 9.6$  Hz, 1H), 6.86 (d,  $J = 8.5$  Hz, 1H), 4.32 (d,  $J = 12.5$  Hz, 1H), 3.39 (d,  $J = 13.5$  Hz, 2H), 1.74 (d,  $J = 4.2$  Hz, 2H), 1.02 (s, 3H), 1.00 (s, 3H);  $^{13}\text{C}$  NMR (150 MHz,  $\text{DMSO-}d_6$ )  $\delta$  (ppm) 178.1, 163.6, 162.0, 152.5, 147.0, 142.8 (d,  $J = 9.6$  Hz),

138.7, 131.5, 130.9, 130.6, 130.3, 125.2, 123.4, 122.9, 121.8, 118.0, 116.0 (t,  $J = 258.4$  Hz), 112.2, 109.6 (d,  $J = 22.2$  Hz), 104.8 (d,  $J = 25.5$  Hz), 69.8, 47.9, 41.3, 25.3, 24.5; MS (ESI)  $m/z$  604.1 [M + H]<sup>+</sup>.

#### 4.2.2 General procedure for the synthesis of compounds 3–6

**Step 1:** To a vial were added intermediates **3a–6a** (1.0 eq), DMAP (20 mol%, 0.2 eq), DIEA (3.0 eq) and DCM (2 mL). After the reaction mixture was cooled to 0 °C by ice-water bath, 3-(trifluoromethyl)benzenesulfonyl chloride (1.2 eq) was subsequently added dropwise. Then the reaction mixture was stirred at room temperature for 12 h. After completion of the reaction, the resulting mixture was diluted with DCM and washed with water. The separated aqueous phase was washed with DCM. The combined organic layers were dried over MgSO<sub>4</sub>, filtered, and concentrated in vacuo. The crude mixture was purified by column chromatography on silica gel (petroleum: ethyl acetate (EA) = 10:1~3:1) to afford the desired products **3b–6b**.

**Step 2:** To a vial were added intermediates **3b–6b** (1.0 eq), 2-(3-(difluoromethoxy)-5-fluorophenyl)-4,4,5,5-tetramethyl-1,3,2-dioxaborolane (1.2 eq), Pd(dppf)Cl<sub>2</sub> (5 mol%, 0.05 eq), X-Phos (10 mol%, 0.1 eq), K<sub>2</sub>CO<sub>3</sub> (3.0 eq) and 1,4-dioxane (3 mL). Then the reaction mixture was stirred under N<sub>2</sub> atmosphere at 100 °C for 12 h. After completion of the reaction, the resulting mixture was diluted with EA and washed with water. The separated aqueous phase was washed with EA. The combined organic layers were dried over MgSO<sub>4</sub>, filtered, and concentrated in vacuo. The crude mixture was purified by column chromatography on silica gel (petroleum: EA = 10:1~5:1) to afford the desired products **3–6**.

##### 4.2.2.1 6-(3-(Difluoromethoxy)-5-fluorophenyl)-1-((3-(trifluoromethyl)phenyl)sulfonyl)indoline (**3**).

Yield: 52%, white solid, purity: 94%. <sup>1</sup>H NMR (400 MHz, DMSO-*d*<sub>6</sub>) δ (ppm) 8.15 (d,  $J = 6.6$  Hz, 1H), 8.04 (s, 2H), 7.79 (t,  $J = 7.2$  Hz, 1H), 7.63 (s, 1H), 7.58 – 7.39 (m, 1H), 7.32 (d,  $J = 5.1$  Hz, 2H), 7.24 – 7.19 (m, 2H), 7.13 (d,  $J = 8.9$  Hz, 1H), 4.00 (t,  $J = 6.6$  Hz, 2H), 2.88 (t,  $J = 7.3$  Hz, 2H); <sup>13</sup>C NMR (150 MHz, DMSO-*d*<sub>6</sub>) δ (ppm) 163.5, 161.9, 152.2 (d,  $J = 12.0$  Hz), 143.4 (d,  $J = 9.5$  Hz), 141.6, 137.7, 137.2, 133.1, 131.2, 131.0, 130.4, 129.9 (d,  $J = 32.9$  Hz), 126.1, 123.5, 123.3, 116.1 (t,  $J = 258.4$  Hz), 112.8, 112.3, 110.2 (d,  $J = 22.3$  Hz), 105.3 (d,  $J = 25.6$  Hz), 50.4, 26.9; MS (ESI)  $m/z$  488.1 [M + H]<sup>+</sup>.

4.2.2.2 6-(3-(Difluoromethoxy)-5-fluorophenyl)-1-((3-(trifluoromethyl)phenyl)sulfonyl)-1H-indole (4). Yield: 48%, white solid, purity: 98%.  $^1\text{H}$  NMR (400 MHz, DMSO- $d_6$ )  $\delta$  (ppm) 8.45 (s, 1H), 8.41 (d,  $J = 7.2$  Hz, 1H), 8.18 (s, 1H), 8.10 (d,  $J = 6.7$  Hz, 1H), 8.02 (s, 1H), 7.84 (t,  $J = 7.1$  Hz, 1H), 7.72 (d,  $J = 7.6$  Hz, 1H), 7.63 (d,  $J = 7.7$  Hz, 1H), 7.46 (d,  $J = 8.0$  Hz, 2H), 7.30 (d,  $J = 14.8$  Hz, 2H), 7.17 (d,  $J = 9.4$  Hz, 1H), 6.94 (s, 1H);  $^{13}\text{C}$  NMR (150 MHz, DMSO- $d_6$ )  $\delta$  (ppm) 163.5, 161.9, 152.2 (d,  $J = 11.9$  Hz), 143.6 (d,  $J = 9.5$  Hz), 137.8, 135.0, 134.5, 131.5, 131.3, 130.8, 130.7, 130.2 (d,  $J = 33.0$  Hz), 128.1, 123.4, 123.2, 122.3, 116.1 (t,  $J = 258.2$  Hz), 113.0, 111.0, 110.6 (d,  $J = 22.3$  Hz), 110.0, 105.1 (d,  $J = 25.6$  Hz); MS (ESI)  $m/z$  486.1  $[\text{M} + \text{H}]^+$ .

#### 4.2.2.3

6-(3-(Difluoromethoxy)-5-fluorophenyl)-1-((3-(trifluoromethyl)phenyl)sulfonyl)-1H-indazole (5). Yield: 42%, white solid, purity: 98%.  $^1\text{H}$  NMR (400 MHz, DMSO- $d_6$ )  $\delta$  (ppm) 8.10 (d,  $J = 7.7$  Hz, 1H), 8.00 (d,  $J = 8.7$  Hz, 2H), 7.95 (d,  $J = 8.1$  Hz, 1H), 7.85 (d,  $J = 7.8$  Hz, 1H), 7.81 (d,  $J = 8.9$  Hz, 1H), 7.57 – 7.39 (m, 1H), 7.33 (s, 1H), 7.31 – 7.21 (m, 2H), 7.16 (s, 1H);  $^{13}\text{C}$  NMR (150 MHz, DMSO- $d_6$ )  $\delta$  (ppm) 170.1, 163.5, 161.9, 152.3 (d,  $J = 12.0$  Hz), 142.9, 140.7 (d,  $J = 9.6$  Hz), 140.4, 138.6, 134.5, 131.0, 130.7, 129.8, 126.0, 125.3, 123.3, 115.9, 115.8 (t,  $J = 258.8$  Hz), 113.0, 110.5 (d,  $J = 22.9$  Hz), 109.8, 106.8 (d,  $J = 25.6$  Hz); MS (ESI)  $m/z$  487.1  $[\text{M} + \text{H}]^+$ .

#### 4.2.2.4

6-(3-(Difluoromethoxy)-5-fluorophenyl)-1-((3-(trifluoromethyl)phenyl)sulfonyl)-1H-benzo[d]imidazole (6). Yield: 43%, white solid, purity: 99%.  $^1\text{H}$  NMR (400 MHz,  $\text{CDCl}_3$ )  $\delta$  (ppm) 8.43 (s, 1H), 8.32 (s, 1H), 8.20 (d,  $J = 8.0$  Hz, 1H), 7.99 (d,  $J = 1.3$  Hz, 1H), 7.93 (d,  $J = 7.8$  Hz, 1H), 7.86 (d,  $J = 8.4$  Hz, 1H), 7.73 (t,  $J = 7.9$  Hz, 1H), 7.57 (dd,  $J = 8.4, 1.7$  Hz, 1H), 7.18 – 7.14 (m, 2H), 6.94 – 6.90 (m, 1H), 6.60 (t,  $J = 73.0$  Hz, 1H);  $^{13}\text{C}$  NMR (150 MHz, DMSO- $d_6$ )  $\delta$  (ppm) 163.5, 161.9, 152.2 (d,  $J = 12.3$  Hz), 143.5 (d,  $J = 10.7$  Hz), 143.1 (d,  $J = 9.7$  Hz), 137.6, 136.0, 132.1, 131.8, 131.5, 130.6 (t,  $J = 16.7$  Hz), 124.6, 124.3, 123.7, 121.9, 121.2, 116.1 (t,  $J = 258.3$  Hz), 113.3, 110.9 (d,  $J = 22.5$  Hz), 110.3, 105.4 (d,  $J = 25.8$  Hz); MS (ESI)  $m/z$  487.1  $[\text{M} + \text{H}]^+$ .

#### 4.2.3 General procedure for the synthesis of compounds 7–19

**Step 1:** To a vial were added intermediates **7a–19a** (1.0 eq), DMAP (20 mol%, 0.2 eq), DIEA (3.0 eq) and DCM (2 mL). After the reaction mixture was cooled to 0 °C by ice-water bath, 3-(trifluoromethyl)benzenesulfonyl chloride (1.2 eq) was subsequently added dropwise. Then the reaction mixture was stirred at room temperature for 12 h. After completion of the reaction, the resulting mixture was diluted with DCM and washed with water. The separated aqueous phase was washed with DCM. The combined organic layers were dried over MgSO<sub>4</sub>, filtered, and concentrated in vacuo. The crude mixture was purified by column chromatography on silica gel (petroleum: EA = 10:1~3:1) to afford the desired products **7b–19b**.

**Step 2:** To a vial were added intermediates **7b–19b** (1.0 eq), 2-(3-(difluoromethoxy)-5-fluorophenyl)-4,4,5,5-tetramethyl-1,3,2-dioxaborolane (1.2 eq), Pd(dppf)Cl<sub>2</sub> (5 mol%, 0.05 eq), X-Phos (10 mol%, 0.1 eq), K<sub>2</sub>CO<sub>3</sub> (3.0 eq) and 1,4-dioxane (3 mL). Then the reaction mixture was stirred under N<sub>2</sub> atmosphere at 100 °C for 12 h. After completion of the reaction, the resulting mixture was diluted with EA and washed with water. The separated aqueous phase was washed with EA. The combined organic layers were dried over MgSO<sub>4</sub>, filtered, and concentrated in vacuo. The crude mixture was purified by column chromatography on silica gel (petroleum: EA = 10:1~5:1) to afford the desired products **7c–19c**.

**Step 3:** To a vial were added intermediates **7c–19c** (1.0 eq), LiOH aq. (2*N*, 2.0 eq) and THF (2 mL). After that the reaction mixture was stirred at room temperature for 5 h. After completion of the reaction, the pH of solution was adjusted to about 3 by HCl (2*N*). Then the resulting mixture was diluted with EA and washed with water. The separated aqueous phase was washed with EA. The combined organic layers were dried over MgSO<sub>4</sub>, filtered, and concentrated in vacuo. The crude mixture was purified by column chromatography on silica gel (petroleum: EA = 1:1~1:8) to afford the desired products **7–19**.

#### 4.2.3.1

*6-(3-(Difluoromethoxy)-5-fluorophenyl)-1-((3-(trifluoromethyl)phenyl)sulfonyl)-1H-indole-2-carboxylic acid (7)*. Yield: 76%, white solid, purity: 97%. <sup>1</sup>H NMR (400 MHz, CD<sub>3</sub>OD) δ (ppm) 8.38 (s, 1H), 8.30 (s, 2H), 7.96 (d, *J* = 7.6 Hz, 1H), 7.75 (t, *J* = 8.0 Hz, 1H), 7.71 (d, *J* = 8.3 Hz, 1H), 7.58 (d, *J* = 8.1 Hz, 1H), 7.30 (d, *J* = 10.3 Hz, 1H), 7.26 (d, *J* = 7.1 Hz, 2H), 7.00 (s, 1H), 6.89 (t, *J* = 64.7 Hz, 1H); <sup>13</sup>C NMR (150 MHz, CD<sub>3</sub>OD) δ (ppm) 163.6, 162.0, 152.2 (d, *J* = 11.6 Hz), 143.8

(d,  $J = 9.4$  Hz), 138.9, 137.8, 137.4, 130.4 (d,  $J = 33.4$  Hz), 129.9, 129.8 (d,  $J = 2.7$  Hz), 129.6, 128.2, 123.6, 123.5, 123.0, 122.4, 121.7, 115.6 (t,  $J = 258.9$  Hz), 115.4, 112.9, 112.8, 109.9 (d,  $J = 22.7$  Hz), 104.8 (d,  $J = 25.6$  Hz); MS (ESI)  $m/z$  530.1  $[M + H]^+$ .

#### 4.2.3.2

*2-(6-(3-(Difluoromethoxy)-5-fluorophenyl)-1-((3-(trifluoromethyl)phenyl)sulfonyl)-1H-indol-2-yl)acetic acid (8)*. Yield: 73%, pale yellow solid, purity: 93%.  $^1\text{H}$  NMR (400 MHz,  $\text{CDCl}_3$ )  $\delta$  (ppm) 8.20 (s, 1H), 8.08 (s, 1H), 8.00 (d,  $J = 8.0$  Hz, 1H), 7.82 (d,  $J = 8.0$  Hz, 1H), 7.62 (d,  $J = 7.7$  Hz, 1H), 7.56 (d,  $J = 8.1$  Hz, 1H), 7.43 (d,  $J = 8.2$  Hz, 1H), 7.11 (d,  $J = 14.8$  Hz, 2H), 6.87 (d,  $J = 9.1$  Hz, 1H), 6.68 (s, 1H), 6.58 (t,  $J = 73.2$  Hz, 1H), 4.19 (s, 2H);  $^{13}\text{C}$  NMR (150 MHz,  $\text{CDCl}_3$ )  $\delta$  (ppm) 174.3, 164.1, 162.5, 152.1 (d,  $J = 9.0$  Hz), 144.5 (d,  $J = 9.3$  Hz), 139.7, 137.0, 136.3, 133.9, 130.7 (d,  $J = 2.6$  Hz), 130.3, 129.9, 129.2, 124.0 (d,  $J = 3.3$  Hz), 123.5, 121.6, 115.6 (t,  $J = 261.5$  Hz), 114.3, 113.0, 112.8, 111.4 (d,  $J = 22.2$  Hz), 106.2 (d,  $J = 25.1$  Hz), 34.7; MS (ESI)  $m/z$  544.1  $[M + H]^+$ .

#### 4.2.3.3

*3-(6-(3-(Difluoromethoxy)-5-fluorophenyl)-1-((3-(trifluoromethyl)phenyl)sulfonyl)-1H-indol-2-yl)propanoic acid (9)*. Yield: 78%, pale yellow solid, purity: 98%.  $^1\text{H}$  NMR (400 MHz,  $\text{CDCl}_3$ )  $\delta$  (ppm) 8.29 (s, 1H), 8.10 (s, 1H), 7.90 (d,  $J = 6.4$  Hz, 1H), 7.80 (d,  $J = 6.3$  Hz, 1H), 7.58 (t,  $J = 6.9$  Hz, 1H), 7.50 (d,  $J = 7.3$  Hz, 1H), 7.43 (d,  $J = 7.4$  Hz, 1H), 7.17 (d,  $J = 13.3$  Hz, 2H), 6.88 (d,  $J = 7.8$  Hz, 1H), 6.69 (t,  $J = 73.7$  Hz, 1H), 6.52 (s, 1H), 3.37 (d,  $J = 16.9$  Hz, 2H), 2.88 (d,  $J = 17.8$  Hz, 2H);  $^{13}\text{C}$  NMR (150 MHz,  $\text{CDCl}_3$ )  $\delta$  (ppm) 176.2, 164.1, 162.5, 152.2 (d,  $J = 11.5$  Hz), 144.7 (d,  $J = 9.3$  Hz), 141.1, 139.7, 137.6, 136.0, 132.1 (d,  $J = 33.7$  Hz), 130.6, 130.3, 130.0, 129.7 (d,  $J = 5.8$  Hz), 129.4, 123.6, 121.1, 115.7 (t,  $J = 261.5$  Hz), 114.3, 113.3, 111.4 (d,  $J = 22.1$  Hz), 109.9, 106.1 (d,  $J = 25.1$  Hz), 32.9, 24.9; MS (ESI)  $m/z$  558.1  $[M + H]^+$ .

#### 4.2.3.4

*4-(6-(3-(Difluoromethoxy)-5-fluorophenyl)-1-((3-(trifluoromethyl)phenyl)sulfonyl)-1H-indol-2-yl)butanoic acid (10)*. Yield: 71%, white solid, purity: 96%.  $^1\text{H}$  NMR (400 MHz,  $\text{CDCl}_3$ )  $\delta$  (ppm) 8.31 (s, 1H), 8.08 (s, 1H), 7.82 (dd,  $J = 21.7, 7.8$  Hz, 2H), 7.57 (t,  $J = 7.9$  Hz, 1H), 7.50 (d,  $J = 8.1$

Hz, 1H), 7.42 (d,  $J = 8.1$  Hz, 1H), 7.18 (d,  $J = 13.2$  Hz, 2H), 6.86 (d,  $J = 9.1$  Hz, 1H), 6.69 (t,  $J = 73.3$  Hz, 1H), 6.51 (s, 1H), 3.11 (t,  $J = 7.4$  Hz, 2H), 2.50 (t,  $J = 7.1$  Hz, 2H), 2.18 – 2.11 (m, 2H);  $^{13}\text{C}$  NMR (150 MHz,  $\text{CDCl}_3$ )  $\delta$  (ppm) 177.6, 164.1, 162.5, 152.2 (d,  $J = 11.6$  Hz), 144.8 (d,  $J = 9.3$  Hz), 142.1, 139.8, 137.7, 135.8, 132.1 (d,  $J = 34.1$  Hz), 130.5, 130.3, 129.9, 129.3, 123.5, 123.4 (d,  $J = 3.1$  Hz), 121.0, 115.8 (t,  $J = 261.4$  Hz), 114.3, 113.4, 111.4 (d,  $J = 22.1$  Hz), 110.1, 106.1 (d,  $J = 25.3$  Hz), 32.9, 28.4, 23.9; MS (ESI)  $m/z$  572.1  $[\text{M} + \text{H}]^+$ .

#### 4.2.3.5

2-(6-(3-(Difluoromethoxy)-5-fluorophenyl)-1-((3-(trifluoromethyl)phenyl)sulfonyl)-1H-indol-3-yl)acetic acid (**11**). Yield: 75%, pale yellow solid, purity: 95%.  $^1\text{H}$  NMR (400 MHz,  $\text{CDCl}_3$ )  $\delta$  (ppm) 8.19 (s, 1H), 8.12 (s, 1H), 8.07 (d,  $J = 7.4$  Hz, 1H), 7.81 (d,  $J = 6.2$  Hz, 1H), 7.65 (s, 1H), 7.62 – 7.57 (m, 2H), 7.46 (d,  $J = 7.4$  Hz, 1H), 7.15 (d,  $J = 10.1$  Hz, 2H), 6.89 (d,  $J = 8.4$  Hz, 1H), 6.60 (t,  $J = 73.3$  Hz, 1H), 3.78 (s, 2H);  $^{13}\text{C}$  NMR (150 MHz,  $\text{CDCl}_3$ )  $\delta$  (ppm) 175.7, 164.1, 162.5, 152.2 (d,  $J = 11.5$  Hz), 144.3 (d,  $J = 9.2$  Hz), 139.0, 136.8, 135.4, 132.1 (q,  $J = 33.9$  Hz), 130.7 (d,  $J = 2.6$  Hz), 130.4, 130.4, 129.9, 125.7, 123.9 (d,  $J = 3.2$  Hz), 123.3, 120.3, 115.6 (t,  $J = 261.5$  Hz), 115.4, 114.4, 112.1, 111.5 (d,  $J = 22.2$  Hz), 106.3 (d,  $J = 25.2$  Hz), 60.5; MS (ESI)  $m/z$  544.1  $[\text{M} + \text{H}]^+$ .

#### 4.2.3.6

3-(6-(3-(Difluoromethoxy)-5-fluorophenyl)-1-((3-(trifluoromethyl)phenyl)sulfonyl)-1H-indol-3-yl)propanoic acid (**12**). Yield: 76%, pale yellow solid, purity: 94%.  $^1\text{H}$  NMR (400 MHz,  $\text{CDCl}_3$ )  $\delta$  (ppm) 8.17 (s, 1H), 8.12 (s, 1H), 8.03 (d,  $J = 7.4$  Hz, 1H), 7.80 (d,  $J = 7.8$  Hz, 1H), 7.59 (dd,  $J = 13.6, 8.1$  Hz, 2H), 7.46 (d,  $J = 10.7$  Hz, 2H), 7.16 (d,  $J = 14.3$  Hz, 2H), 6.89 (d,  $J = 9.0$  Hz, 1H), 6.60 (t,  $J = 73.2$  Hz, 1H), 3.05 (t,  $J = 7.2$  Hz, 2H), 2.78 (t,  $J = 7.3$  Hz, 2H);  $^{13}\text{C}$  NMR (150 MHz,  $\text{CDCl}_3$ )  $\delta$  (ppm) 175.7, 164.3, 162.7, 152.2 (d,  $J = 10.5$  Hz), 144.4 (d,  $J = 9.0$  Hz), 139.2, 136.7, 135.7, 132.3, 132.0, 130.7, 130.6 (d,  $J = 2.6$  Hz), 130.3, 129.8, 123.9, 123.1, 122.3, 120.1, 115.6 (t,  $J = 261.7$  Hz), 114.4, 112.3, 111.5 (d,  $J = 22.2$  Hz), 106.3 (d,  $J = 25.1$  Hz), 32.9, 20.0; MS (ESI)  $m/z$  558.1  $[\text{M} + \text{H}]^+$ .

#### 4.2.3.7

4-(6-(3-(Difluoromethoxy)-5-fluorophenyl)-1-((3-(trifluoromethyl)phenyl)sulfonyl)-1H-indol-3-yl)

*butanoic acid (13)*. Yield: 72%, white solid, purity: 96%.  $^1\text{H}$  NMR (400 MHz,  $\text{CDCl}_3$ )  $\delta$  (ppm) 8.17 (s, 1H), 8.13 (s, 1H), 8.05 (d,  $J = 6.4$  Hz, 1H), 7.81 (d,  $J = 6.3$  Hz, 1H), 7.60 (dd,  $J = 17.4, 8.0$  Hz, 2H), 7.45 – 7.41 (m, 2H), 7.16 (d,  $J = 10.9$  Hz, 2H), 6.88 (d,  $J = 7.8$  Hz, 1H), 6.61 (t,  $J = 73.2$  Hz, 1H), 2.77 (t,  $J = 7.1$  Hz, 2H), 2.42 (t,  $J = 6.8$  Hz, 2H), 2.12 – 1.98 (m, 2H);  $^{13}\text{C}$  NMR (150 MHz,  $\text{CDCl}_3$ )  $\delta$  (ppm) 178.5, 164.1, 162.5, 152.2 (d,  $J = 11.7$  Hz), 144.5 (d,  $J = 9.2$  Hz), 139.1, 136.5, 135.8, 132.1 (q,  $J = 33.9$  Hz), 131.0, 130.6 (d,  $J = 2.7$  Hz), 130.3, 129.8, 123.8 (d,  $J = 3.3$  Hz), 123.7, 123.1, 123.1, 120.3, 115.6 (t,  $J = 261.5$  Hz), 114.4, 112.2, 111.5 (d,  $J = 22.2$  Hz), 106.2 (d,  $J = 25.2$  Hz), 33.1, 24.1, 23.8; MS (ESI)  $m/z$  572.1  $[\text{M} + \text{H}]^+$ .

#### 4.2.3.8

*2-(6-(3-(Difluoromethoxy)-5-fluorophenyl)-1-((3-(trifluoromethyl)phenyl)sulfonyl)indolin-2-yl)acetic acid (14)*. Yield: 76%, white solid, purity: 99%.  $^1\text{H}$  NMR (400 MHz,  $\text{CDCl}_3$ )  $\delta$  (ppm) 7.96 (s, 1H), 7.90 (d,  $J = 8.1$  Hz, 1H), 7.85 – 7.81 (m, 2H), 7.59 (t,  $J = 7.6$  Hz, 1H), 7.17 – 7.13 (m, 4H), 6.89 (d,  $J = 9.0$  Hz, 1H), 6.59 (t,  $J = 73.1$  Hz, 1H), 4.65 (t,  $J = 9.5$  Hz, 1H), 3.17 (dd,  $J = 16.2, 3.6$  Hz, 1H), 3.02 (dd,  $J = 16.7, 9.3$  Hz, 1H), 2.81 – 2.71 (m, 2H);  $^{13}\text{C}$  NMR (150 MHz,  $\text{CDCl}_3$ )  $\delta$  (ppm) 174.4, 164.1, 162.5, 152.2 (d,  $J = 11.2$  Hz), 143.9 (d,  $J = 9.1$  Hz), 141.3, 139.6, 138.8, 131.9 (d,  $J = 33.5$  Hz), 131.3, 130.1 (d,  $J = 4.2$  Hz), 126.0, 124.5, 124.2 (d,  $J = 3.2$  Hz), 123.9, 122.0, 115.6 (t,  $J = 261.7$  Hz), 115.5, 114.1, 111.3 (d,  $J = 22.2$  Hz), 106.5 (d,  $J = 25.3$  Hz), 59.3, 41.0, 34.5; HRMS (ESI):  $m/z$   $[\text{M} + \text{H}]^+$  calcd for  $\text{C}_{24}\text{H}_{18}\text{F}_6\text{NO}_5\text{S}$ : 546.0804, found: 546.0809.

#### 4.2.3.9

*3-(6-(3-(Difluoromethoxy)-5-fluorophenyl)-1-((3-(trifluoromethyl)phenyl)sulfonyl)indolin-2-yl)propanoic acid (15)*. Yield: 77%, white solid, purity: 96%.  $^1\text{H}$  NMR (400 MHz,  $\text{CDCl}_3$ )  $\delta$  (ppm) 7.84 (d,  $J = 6.6$  Hz, 2H), 7.79 (t,  $J = 6.1$  Hz, 2H), 7.54 (t,  $J = 7.8$  Hz, 1H), 7.27 (d,  $J = 7.3$  Hz, 1H), 7.16 (t,  $J = 12.6$  Hz, 3H), 6.89 (d,  $J = 8.9$  Hz, 1H), 6.60 (t,  $J = 73.2$  Hz, 1H), 4.45 (d,  $J = 7.0$  Hz, 1H), 2.80 – 2.71 (m, 1H), 2.68 – 2.59 (m, 2H), 2.49 (d,  $J = 16.4$  Hz, 1H), 1.98 (dd,  $J = 16.3, 9.7$  Hz, 2H);  $^{13}\text{C}$  NMR (150 MHz,  $\text{CDCl}_3$ )  $\delta$  (ppm) 175.6, 164.3, 162.6, 152.3 (d,  $J = 10.8$  Hz), 143.8 (d,  $J = 9.4$  Hz), 141.3, 139.3, 138.9, 133.0, 130.1, 129.8, 125.8, 124.9, 124.1, 117.2, 115.6 (t,  $J = 259.5$  Hz), 114.1, 111.3 (d,  $J = 22.4$  Hz), 106.5 (d,  $J = 24.7$  Hz), 62.3, 34.5, 30.9, 29.7; MS (ESI)  $m/z$  560.1  $[\text{M} + \text{H}]^+$ .

## 4.2.3.10

4-(6-(3-(Difluoromethoxy)-5-fluorophenyl)-1-((3-(trifluoromethyl)phenyl)sulfonyl)indolin-2-yl)butanoic acid (**16**). Yield: 74%, white solid, purity: 97%.  $^1\text{H}$  NMR (400 MHz,  $\text{CDCl}_3$ )  $\delta$  (ppm) 7.89 (s, 1H), 7.84 – 7.74 (m, 3H), 7.55 (t,  $J = 6.6$  Hz, 1H), 7.26 (d,  $J = 5.7$  Hz, 1H), 7.12 (q,  $J = 14.8$  Hz, 3H), 6.88 (d,  $J = 8.0$  Hz, 1H), 6.60 (t,  $J = 72.5$  Hz, 1H), 4.32 (t,  $J = 10.4$  Hz, 1H), 2.72 (dd,  $J = 15.9, 8.8$  Hz, 1H), 2.55 (d,  $J = 16.4$  Hz, 1H), 2.44 – 2.35 (m, 2H), 1.83 – 1.63 (m, 4H);  $^{13}\text{C}$  NMR (150 MHz,  $\text{CDCl}_3$ )  $\delta$  (ppm) 179.0, 164.1, 162.5, 152.2 (d,  $J = 11.6$  Hz), 143.9 (d,  $J = 9.2$  Hz), 141.6, 139.3, 139.1, 132.9, 131.7 (q,  $J = 33.5$  Hz), 130.0, 129.9, 129.7 (d,  $J = 2.4$  Hz), 125.8, 124.6, 124.1, 124.1, 116.5, 115.6 (t,  $J = 259.5$  Hz), 114.1, 111.2 (d,  $J = 22.2$  Hz), 106.4 (d,  $J = 25.2$  Hz), 63.0, 35.7, 34.0, 33.4, 20.2; MS (ESI)  $m/z$  574.1  $[\text{M} + \text{H}]^+$ .

## 4.2.3.11

2-(6-(3-(Difluoromethoxy)-5-fluorophenyl)-1-((3-(trifluoromethyl)phenyl)sulfonyl)indolin-3-yl)acetic acid (**17**). Yield: 75%, pale yellow solid, purity: 94%.  $^1\text{H}$  NMR (400 MHz,  $\text{CDCl}_3$ )  $\delta$  (ppm) 8.12 (s, 1H), 8.00 (d,  $J = 7.6$  Hz, 1H), 7.86 (d,  $J = 7.3$  Hz, 1H), 7.81 (s, 1H), 7.65 (t,  $J = 7.9$  Hz, 1H), 7.20 (d,  $J = 3.7$  Hz, 2H), 7.14 (dd,  $J = 17.3, 8.0$  Hz, 2H), 6.90 (d,  $J = 9.0$  Hz, 1H), 6.59 (t,  $J = 73.0$  Hz, 1H), 4.24 – 4.19 (m, 1H), 3.81 (dd,  $J = 11.1, 5.6$  Hz, 1H), 3.65 – 3.58 (m, 1H), 2.66 (dd,  $J = 17.2, 4.6$  Hz, 1H), 2.30 (dd,  $J = 16.9, 9.9$  Hz, 1H);  $^{13}\text{C}$  NMR (150 MHz,  $\text{CDCl}_3$ )  $\delta$  (ppm) 175.5, 164.1, 162.5, 152.2 (d,  $J = 11.2$  Hz), 143.9 (d,  $J = 9.2$  Hz), 142.0, 140.3, 138.1, 133.8, 132.0 (d,  $J = 33.6$  Hz), 130.2 (d,  $J = 9.5$  Hz), 125.0, 124.4, 123.9, 123.6, 122.1, 115.6 (t,  $J = 261.7$  Hz), 114.2, 113.5, 111.3 (d,  $J = 22.2$  Hz), 106.6 (d,  $J = 25.1$  Hz), 56.1, 38.8, 36.0; MS (ESI)  $m/z$  546.1  $[\text{M} + \text{H}]^+$ .

## 4.2.3.12

3-(6-(3-(Difluoromethoxy)-5-fluorophenyl)-1-((3-(trifluoromethyl)phenyl)sulfonyl)indolin-3-yl)propanoic acid (**18**). Yield: 78%, pale yellow solid, purity: 96%.  $^1\text{H}$  NMR (400 MHz,  $\text{CDCl}_3$ )  $\delta$  (ppm) 8.12 (s, 1H), 8.00 (d,  $J = 7.7$  Hz, 1H), 7.85 (d,  $J = 7.5$  Hz, 1H), 7.79 (s, 1H), 7.64 (t,  $J = 7.8$  Hz, 1H), 7.20 (s, 2H), 7.13 (d,  $J = 14.1$  Hz, 2H), 6.89 (d,  $J = 9.4$  Hz, 1H), 6.59 (t,  $J = 73.2$  Hz, 1H), 4.06 (t,  $J = 9.8$  Hz, 1H), 3.71 (dd,  $J = 10.4, 4.8$  Hz, 1H), 3.30 – 3.23 (m, 1H), 2.33 (t,  $J = 7.3$  Hz,

2H), 2.05 – 1.87 (m, 2H); MS (ESI)  $m/z$  560.1  $[M + H]^+$ .

#### 4.2.3.13

*4-(6-(3-(Difluoromethoxy)-5-fluorophenyl)-1-((3-(trifluoromethyl)phenyl)sulfonyl)indolin-3-yl)butanoic acid (19)*. Yield: 79%, white solid, purity: 97%.  $^1\text{H}$  NMR (400 MHz,  $\text{CDCl}_3$ )  $\delta$  (ppm) 8.12 (s, 1H), 8.01 (d,  $J = 6.7$  Hz, 1H), 7.84 (d,  $J = 6.8$  Hz, 1H), 7.79 (s, 1H), 7.64 (t,  $J = 6.7$  Hz, 1H), 7.19 – 7.12 (m, 4H), 6.88 (d,  $J = 9.0$  Hz, 1H), 6.59 (t,  $J = 73.2$  Hz, 1H), 4.10 (t,  $J = 9.4$  Hz, 1H), 3.73 – 3.70 (m, 1H), 3.21 (s, 1H), 2.33 (s, 2H), 1.62 (s, 4H);  $^{13}\text{C}$  NMR (150 MHz,  $\text{CDCl}_3$ )  $\delta$  (ppm) 178.6, 164.0, 162.4, 152.1 (d,  $J = 11.5$  Hz), 144.0 (d,  $J = 9.1$  Hz), 141.9, 139.6, 138.0, 135.2, 131.8 (q,  $J = 33.6$  Hz), 130.2, 130.1, 130.0, 125.1, 124.3, 123.3, 115.6 (t,  $J = 261.4$  Hz), 114.0, 113.1, 111.2 (d,  $J = 22.2$  Hz), 106.4 (d,  $J = 25.2$  Hz), 55.8, 39.5, 34.0, 33.5, 24.7; MS (ESI)  $m/z$  574.1  $[M + H]^+$ .

#### 4.2.4 General procedure for the synthesis of compounds 20–29

To a vial were added **14** (1.0 eq), related secondary amine (1.2 eq), HATU (1.2 eq), DIEA (3.0 eq) and DCM (2 mL). Then the reaction mixture was stirred at 30 °C for 3-12 h. After completion of the reaction, the resulting mixture was diluted with DCM and washed with water. The separated aqueous phase was washed with DCM. The combined organic layers were dried over  $\text{MgSO}_4$ , filtered, and concentrated in vacuo. The crude mixture was purified by column chromatography on silica gel (petroleum: EA = 8:1~1:1) to afford the desired products **20–29**.

##### 4.2.4.1

*1-(2-(6-(3-(Difluoromethoxy)-5-fluorophenyl)-1-((3-(trifluoromethyl)phenyl)sulfonyl)indolin-2-yl)acetyl)azetidin-3-one (20)*. Yield: 80%, white solid, purity: 96%.  $^1\text{H}$  NMR (400 MHz,  $\text{CDCl}_3$ )  $\delta$  (ppm) 7.95 (s, 1H), 7.91 (d,  $J = 8.1$  Hz, 1H), 7.84 (s, 1H), 7.82 (d,  $J = 7.6$  Hz, 1H), 7.60 (t,  $J = 7.7$  Hz, 1H), 7.15 (dd,  $J = 13.9, 5.7$  Hz, 4H), 6.89 (d,  $J = 9.0$  Hz, 1H), 6.59 (t,  $J = 73.3$  Hz, 1H), 4.99 (d,  $J = 14.9$  Hz, 1H), 4.87 (d,  $J = 19.0$  Hz, 2H), 4.73 (d,  $J = 13.8$  Hz, 2H), 3.10 – 3.02 (m, 2H), 2.85 (dd,  $J = 12.4, 5.9$  Hz, 1H), 2.69 (dd,  $J = 15.5, 8.8$  Hz, 1H);  $^{13}\text{C}$  NMR (150 MHz,  $\text{CDCl}_3$ )  $\delta$  (ppm) 193.8, 169.6, 165.8, 164.1, 162.5, 152.2 (d,  $J = 11.5$  Hz), 143.8 (d,  $J = 9.3$  Hz), 141.3, 139.6, 138.4, 131.5, 130.1, 126.1, 124.5, 124.2, 123.8, 122.0, 115.6 (t,  $J = 261.6$  Hz), 115.1, 114.1,

111.2 (d,  $J = 22.3$  Hz), 106.5 (d,  $J = 25.1$  Hz), 59.9, 40.2, 38.6, 34.6; MS (ESI)  $m/z$  599.1 [ $M + H$ ]<sup>+</sup>.

#### 4.2.4.2

*2-(6-(3-(Difluoromethoxy)-5-fluorophenyl)-1-((3-(trifluoromethyl)phenyl)sulfonyl)indolin-2-yl)-1-(3-hydroxyazetid-1-yl)ethanone (21)*. Yield: 65%, pale yellow solid, purity: 95%. <sup>1</sup>H NMR (400 MHz, CDCl<sub>3</sub>)  $\delta$  (ppm) 7.92 (s, 1H), 7.89 (d,  $J = 6.6$  Hz, 1H), 7.82 (s, 1H), 7.79 (d,  $J = 7.8$  Hz, 1H), 7.58 (t,  $J = 7.2$  Hz, 1H), 7.23 (d,  $J = 8.0$  Hz, 1H), 7.14 (d,  $J = 9.8$  Hz, 3H), 6.87 (d,  $J = 9.0$  Hz, 1H), 6.59 (t,  $J = 73.1$  Hz, 1H), 4.69 – 4.64 (m, 2H), 4.42 – 4.17 (m, 2H), 3.96 (dddd,  $J = 48.9, 37.9, 10.0, 3.8$  Hz, 3H), 3.02 – 2.94 (m, 1H), 2.85 – 2.76 (m, 2H), 2.48 (dd,  $J = 14.9, 9.6$  Hz, 1H); <sup>13</sup>C NMR (150 MHz, CDCl<sub>3</sub>)  $\delta$  (ppm) 169.7 (d,  $J = 28.6$  Hz), 165.8, 164.1, 162.4, 152.1 (d,  $J = 11.4$  Hz), 143.9 (d,  $J = 6.0$  Hz), 141.2, 139.4, 138.6 (d,  $J = 7.8$  Hz), 131.9 (d,  $J = 7.8$  Hz), 130.1 (d,  $J = 2.0$  Hz), 126.1, 124.4 (d,  $J = 4.3$  Hz), 124.1, 123.8, 122.0, 115.6 (t,  $J = 261.4$  Hz), 115.2 (d,  $J = 11.8$  Hz), 114.0, 111.2 (d,  $J = 22.1$  Hz), 106.4 (d,  $J = 26.5$  Hz), 61.1 (d,  $J = 13.0$  Hz), 60.1, 59.9 (d,  $J = 13.0$  Hz), 57.7 (d,  $J = 22.5$  Hz), 38.8 (d,  $J = 5.0$  Hz), 34.5; MS (ESI)  $m/z$  601.1 [ $M + H$ ]<sup>+</sup>.

#### 4.2.4.3

*1-(2-(6-(3-(Difluoromethoxy)-5-fluorophenyl)-1-((3-(trifluoromethyl)phenyl)sulfonyl)indolin-2-yl)acetyl)azetid-3-carboxylic acid (22)*. Yield: 88%, white solid, purity: 97%. <sup>1</sup>H NMR (400 MHz, CDCl<sub>3</sub>)  $\delta$  (ppm) 7.92 – 7.88 (m, 2H), 7.82 (s, 1H), 7.79 (d,  $J = 7.4$  Hz, 1H), 7.57 (t,  $J = 7.5$  Hz, 1H), 7.23 (d,  $J = 8.0$  Hz, 1H), 7.18 – 7.10 (m, 3H), 6.87 (d,  $J = 9.0$  Hz, 1H), 6.59 (t,  $J = 73.2$  Hz, 1H), 4.69 (s, 1H), 4.28 (dd,  $J = 54.5, 29.6$  Hz, 3H), 3.47 – 3.12 (m, 1H), 2.99 – 2.93 (m, 1H), 2.79 (t,  $J = 18.8$  Hz, 2H), 2.47 (dd,  $J = 17.1, 8.5$  Hz, 1H), 2.27 (dd,  $J = 27.8, 21.0$  Hz, 1H); <sup>13</sup>C NMR (150 MHz, CDCl<sub>3</sub>)  $\delta$  (ppm) 170.0, 164.1, 162.4, 152.2 (d,  $J = 11.3$  Hz), 143.9 (d,  $J = 9.1$  Hz), 141.2 (d,  $J = 10.5$  Hz), 139.4, 138.6 (d,  $J = 6.4$  Hz), 131.9, 131.7, 130.1, 130.0, 126.1, 124.5, 124.1, 123.8, 122.0, 115.6 (t,  $J = 261.4$  Hz), 115.3, 114.0, 111.2 (d,  $J = 22.3$  Hz), 106.4 (d,  $J = 24.8$  Hz), 59.9 (d,  $J = 18.4$  Hz), 45.4, 38.4 (d,  $J = 20.2$  Hz), 34.5 (d,  $J = 18.2$  Hz), 31.9; MS (ESI)  $m/z$  629.1 [ $M + H$ ]<sup>+</sup>.

## 4.2.4.4

2-(6-(3-(Difluoromethoxy)-5-fluorophenyl)-1-((3-(trifluoromethyl)phenyl)sulfonyl)indolin-2-yl)-1-(2-oxa-6-azaspiro[3.3]heptan-6-yl)ethanone (**23**). Yield: 71%, white solid, purity: 96%.  $^1\text{H}$  NMR (400 MHz,  $\text{CDCl}_3$ )  $\delta$  (ppm) 7.88 (s, 1H), 7.84 (d,  $J = 7.6$  Hz, 1H), 7.76 (d,  $J = 6.9$  Hz, 2H), 7.55 (t,  $J = 7.5$  Hz, 1H), 7.20 (d,  $J = 7.4$  Hz, 1H), 7.11 – 7.08 (m, 3H), 6.84 (d,  $J = 8.8$  Hz, 1H), 6.57 (t,  $J = 73.2$  Hz, 1H), 4.60 (d,  $J = 8.0$  Hz, 1H), 4.21 (ddd,  $J = 50.4, 38.3, 9.7$  Hz, 3H), 3.62 (d,  $J = 4.5$  Hz, 4H), 2.95 (dd,  $J = 16.9, 9.4$  Hz, 1H), 2.76 (dd,  $J = 22.3, 10.4$  Hz, 2H), 2.41 (dd,  $J = 15.1, 9.0$  Hz, 1H), 2.21 (s, 1H);  $^{13}\text{C}$  NMR (150 MHz,  $\text{CDCl}_3$ )  $\delta$  (ppm) 169.5, 164.0, 162.3, 152.1 (d,  $J = 11.2$  Hz), 143.8 (d,  $J = 9.1$  Hz), 141.1, 139.3, 138.5, 131.8, 130.1, 130.0, 126.0, 124.3, 123.9 (d,  $J = 2.5$  Hz), 123.7, 121.9, 115.5 (t,  $J = 261.5$  Hz), 115.0, 113.9, 111.1 (d,  $J = 22.2$  Hz), 106.3 (d,  $J = 25.3$  Hz), 80.6, 80.5, 59.9, 59.6, 57.3, 38.6, 37.6, 34.5; MS (ESI)  $m/z$  627.1  $[\text{M} + \text{H}]^+$ .

## 4.2.4.5

1-(2-(6-(3-(Difluoromethoxy)-5-fluorophenyl)-1-((3-(trifluoromethyl)phenyl)sulfonyl)indolin-2-yl)acetyl)pyrrolidin-3-one (**24**). Yield: 85%, white solid, purity: 95%.  $^1\text{H}$  NMR (400 MHz,  $\text{CDCl}_3$ )  $\delta$  (ppm) 7.93 (s, 1H), 7.90 (d,  $J = 7.3$  Hz, 1H), 7.84 (d,  $J = 3.3$  Hz, 1H), 7.81 (d,  $J = 7.4$  Hz, 1H), 7.59 (t,  $J = 6.9$  Hz, 1H), 7.23 (s, 1H), 7.16 – 7.13 (m, 3H), 6.88 (d,  $J = 8.9$  Hz, 1H), 6.59 (t,  $J = 73.2$  Hz, 1H), 4.75 (t,  $J = 8.8$  Hz, 1H), 3.97 – 3.82 (m, 4H), 3.19 – 3.02 (m, 2H), 2.84 (dd,  $J = 11.0, 5.6$  Hz, 1H), 2.68 (ddd,  $J = 23.1, 18.5, 8.4$  Hz, 3H);  $^{13}\text{C}$  NMR (150 MHz,  $\text{CDCl}_3$ )  $\delta$  (ppm) 209.0 (d,  $J = 14.6$  Hz), 169.1 (d,  $J = 21.2$  Hz), 165.7, 164.1, 162.4, 152.2 (d,  $J = 11.2$  Hz), 143.8 (d,  $J = 9.1$  Hz), 141.3, 139.5, 138.5, 131.7 (d,  $J = 6.4$  Hz), 130.1, 131.7 (d,  $J = 7.5$  Hz), 124.4, 124.1, 123.8, 122.0, 115.6 (t,  $J = 261.5$  Hz), 115.2 (d,  $J = 17.3$  Hz), 114.1, 111.2 (d,  $J = 22.2$  Hz), 106.5 (d,  $J = 25.2$  Hz), 59.9 (d,  $J = 12.9$  Hz), 52.0, 43.4, 42.0 (d,  $J = 35.5$  Hz), 40.6, 34.9 (d,  $J = 2.7$  Hz); MS (ESI)  $m/z$  613.1  $[\text{M} + \text{H}]^+$ .

## 4.2.4.6

1-(2-(6-(3-(Difluoromethoxy)-5-fluorophenyl)-1-((3-(trifluoromethyl)phenyl)sulfonyl)indolin-2-yl)acetyl)piperidin-4-one (**25**). Yield: 77%, white solid, purity: 94%.  $^1\text{H}$  NMR (400 MHz,  $\text{CDCl}_3$ )  $\delta$  (ppm) 7.95 (s, 1H), 7.91 (d,  $J = 7.9$  Hz, 1H), 7.85 (s, 1H), 7.83 (d,  $J = 7.8$  Hz, 1H), 7.61 (t,  $J = 7.6$  Hz, 1H), 7.29 – 7.25 (m, 1H), 7.18 – 7.13 (m, 3H), 6.90 (d,  $J = 8.6$  Hz, 1H), 6.61 (t,  $J = 73.2$  Hz,

1H), 4.77 (dd,  $J = 12.8, 6.5$  Hz, 1H), 4.05 – 3.99 (m, 1H), 3.87 – 3.63 (m, 3H), 3.22 (dd,  $J = 15.9, 3.0$  Hz, 1H), 3.09 (dd,  $J = 16.5, 9.4$  Hz, 2H), 2.63 – 2.43 (m, 5H);  $^{13}\text{C}$  NMR (150 MHz,  $\text{CDCl}_3$ )  $\delta$  (ppm) 206.2, 168.5, 165.7, 164.1, 162.4, 152.1 (d,  $J = 11.7$  Hz), 143.8 (d,  $J = 9.1$  Hz), 141.3, 139.4, 138.5, 131.8, 130.1 (d,  $J = 11.8$  Hz), 126.1, 124.4, 124.1, 123.8, 122.0, 115.5 (t,  $J = 261.5$  Hz), 115.2, 114.0, 111.2 (d,  $J = 22.2$  Hz), 106.4 (d,  $J = 25.1$  Hz), 60.3, 53.6, 44.0, 38.5, 34.9; MS (ESI)  $m/z$  627.1  $[\text{M} + \text{H}]^+$ .

#### 4.2.4.7

2-(6-(3-(Difluoromethoxy)-5-fluorophenyl)-1-((3-(trifluoromethyl)phenyl)sulfonyl)indolin-2-yl)-1-(4-hydroxypiperidin-1-yl)ethanone (**26**). Yield: 66%, pale yellow solid, purity: 97%.  $^1\text{H}$  NMR (400 MHz,  $\text{CDCl}_3$ )  $\delta$  (ppm) 7.78 (dd,  $J = 7.9, 5.1$  Hz, 2H), 7.70 (d,  $J = 7.3$  Hz, 2H), 7.55 – 7.48 (m, 1H), 7.14 (d,  $J = 7.2$  Hz, 1H), 7.06 – 7.03 (m, 3H), 6.77 (d,  $J = 9.2$  Hz, 1H), 6.54 (t,  $J = 73.2$  Hz, 1H), 4.61 (t,  $J = 9.6$  Hz, 1H), 3.96 – 3.87 (m, 2H), 3.57 – 3.51 (m, 9H), 2.65 – 2.46 (m, 3H);  $^{13}\text{C}$  NMR (150 MHz,  $\text{CDCl}_3$ )  $\delta$  (ppm) 167.6 (d,  $J = 6.4$  Hz), 163.8, 162.2, 151.9 (d,  $J = 11.3$  Hz), 143.8 (d,  $J = 7.9$  Hz), 141.1, 139.0, 138.4, 132.0, 131.5 (d,  $J = 66.0$  Hz), 130.0 (d,  $J = 2.9$  Hz), 129.8 (d,  $J = 11.7$  Hz), 126.0 (d,  $J = 5.8$  Hz), 124.1, 123.7, 121.8, 115.4 (t,  $J = 261.2$  Hz), 115.1, 113.8, 110.9 (d,  $J = 22.1$  Hz), 106.0 (d,  $J = 25.2$  Hz), 66.0 (d,  $J = 22.2$  Hz), 60.3 (d,  $J = 6.0$  Hz), 42.6 (d,  $J = 14.0$  Hz), 40.1 (d,  $J = 4.3$  Hz), 38.7 (d,  $J = 12.9$  Hz), 34.6 (d,  $J = 8.5$  Hz), 34.1 (d,  $J = 15.0$  Hz), 33.4 (d,  $J = 5.5$  Hz); MS (ESI)  $m/z$  629.1  $[\text{M} + \text{H}]^+$ .

#### 4.2.4.8

2-(6-(3-(Difluoromethoxy)-5-fluorophenyl)-1-((3-(trifluoromethyl)phenyl)sulfonyl)indolin-2-yl)-1-morpholinoethanone (**27**). Yield: 78%, white solid, purity: 98%.  $^1\text{H}$  NMR (400 MHz,  $\text{DMSO}-d_6$ )  $\delta$  (ppm) 8.08 (t,  $J = 7.2$  Hz, 2H), 7.90 (s, 1H), 7.82 (t,  $J = 7.3$  Hz, 1H), 7.70 (s, 1H), 7.42 (d,  $J = 6.3$  Hz, 2H), 7.37 (d,  $J = 9.2$  Hz, 1H), 7.26 (d,  $J = 9.5$  Hz, 2H), 7.18 (d,  $J = 9.4$  Hz, 1H), 3.62 – 3.50 (m, 5H), 3.49 – 3.42 (m, 4H), 2.91 (dd,  $J = 18.9, 10.1$  Hz, 3H), 2.71 – 2.65 (m, 1H);  $^{13}\text{C}$  NMR (150 MHz,  $\text{DMSO}-d_6$ )  $\delta$  (ppm) 167.7, 163.5, 161.9, 152.2 (d,  $J = 12.2$  Hz), 143.3 (d,  $J = 9.2$  Hz), 140.8, 137.8, 137.7, 132.7, 131.4, 130.7, 130.5, 129.6 (d,  $J = 21.9$  Hz), 126.4, 124.3, 123.2, 116.0 (t,  $J = 258.5$  Hz), 114.2, 112.7, 110.2 (d,  $J = 22.3$  Hz), 105.3 (d,  $J = 25.5$  Hz), 65.8, 60.3, 45.2, 41.2, 34.1; MS (ESI)  $m/z$  615.1  $[\text{M} + \text{H}]^+$ .

## 4.2.4.9

*1-(2-(6-(3-(Difluoromethoxy)-5-fluorophenyl)-1-((3-(trifluoromethyl)phenyl)sulfonyl)indolin-2-yl)acetyl)piperidine-4-carboxylic acid (28)*. Yield: 86%, white solid, purity: 96%. <sup>1</sup>H NMR (400 MHz, CDCl<sub>3</sub>) δ (ppm) 7.93 (s, 1H), 7.90 (d, *J* = 7.8 Hz, 1H), 7.84 (s, 1H), 7.80 (d, *J* = 7.3 Hz, 1H), 7.58 (t, *J* = 7.2 Hz, 1H), 7.23 (s, 1H), 7.16 – 7.13 (m, 3H), 6.88 (d, *J* = 8.2 Hz, 1H), 6.59 (t, *J* = 73.1 Hz, 1H), 4.77 – 4.69 (m, 1H), 4.39 (dd, *J* = 25.6, 13.1 Hz, 1H), 3.87 – 3.77 (m, 1H), 3.22 – 2.90 (m, 3H), 2.85 – 2.59 (m, 4H), 2.01 (t, *J* = 14.7 Hz, 2H), 1.80 – 1.59 (m, 2H); <sup>13</sup>C NMR (150 MHz, CDCl<sub>3</sub>) δ (ppm) 179.1 (d, *J* = 15.9 Hz), 168.2 (d, *J* = 14.9 Hz), 164.1, 162.5, 152.2 (d, *J* = 11.3 Hz), 143.9 (d, *J* = 9.0 Hz), 141.4, 139.4, 138.7, 132.0, 131.8 (d, *J* = 33.7 Hz), 130.0 (d, *J* = 15.2 Hz), 126.1 (d, *J* = 7.2 Hz), 124.3, 124.1, 123.8, 122.0, 115.6 (d, *J* = 261.5 Hz), 115.3, 114.1, 111.2 (d, *J* = 22.2 Hz), 106.4 (d, *J* = 25.2 Hz), 60.4 (d, *J* = 1.9 Hz), 44.7 (d, *J* = 10.8 Hz), 40.8 (d, *J* = 11.8 Hz), 34.9 (d, *J* = 5.6 Hz), 28.1 (d, *J* = 15.2 Hz), 27.5 (d, *J* = 4.4 Hz); MS (ESI) *m/z* 657.1 [M + H]<sup>+</sup>.

## 4.2.4.10

*2-(6-(3-(Difluoromethoxy)-5-fluorophenyl)-1-((3-(trifluoromethyl)phenyl)sulfonyl)indolin-2-yl)-1-(1,1-dioxidothiomorpholino)ethanone (29)*. Yield: 82%, pale yellow solid, purity: 95%. <sup>1</sup>H NMR (400 MHz, CDCl<sub>3</sub>) δ (ppm) 7.95 (s, 1H), 7.90 (d, *J* = 7.3 Hz, 1H), 7.84 (s, 2H), 7.61 (t, *J* = 6.7 Hz, 1H), 7.27 (d, *J* = 10.2 Hz, 1H), 7.15 (dd, *J* = 9.1, 4.6 Hz, 3H), 6.90 (d, *J* = 8.2 Hz, 1H), 6.62 (t, *J* = 73.2 Hz, 1H), 4.74 (s, 1H), 4.31 – 4.21 (m, 1H), 4.09 – 3.92 (m, 3H), 3.24 – 2.96 (m, 8H); <sup>13</sup>C NMR (150 MHz, CDCl<sub>3</sub>) δ (ppm) 168.5, 165.7, 164.1, 162.4, 152.2 (d, *J* = 11.3 Hz), 143.6 (d, *J* = 9.1 Hz), 141.1, 139.6, 138.3, 131.8 (d, *J* = 33.6 Hz), 131.6, 130.2, 130.0, 126.1, 124.5, 124.1, 115.6 (d, *J* = 261.5 Hz), 115.1, 114.0, 111.2 (d, *J* = 22.2 Hz), 106.5 (d, *J* = 25.2 Hz), 60.2, 51.8 (d, *J* = 17.3 Hz), 44.0, 40.1 (d, *J* = 12.4 Hz), 34.8; MS (ESI) *m/z* 663.1 [M + H]<sup>+</sup>.

## 4.2.5 The synthesis of compounds 30–39

**Step 1:** To a vial were added intermediate **14b** (1.0 eq), bis(pinacolato)diboron (1.2 eq), Pd(dppf)Cl<sub>2</sub> (5 mol%, 0.05 eq), KOAc (3.0 eq) and 1,4-dioxane (3 mL). Then the reaction mixture was stirred under N<sub>2</sub> atmosphere at 100 °C for 12 h. After completion of the reaction, the resulting

mixture was diluted with EA and washed with water. The separated aqueous phase was washed with EA. The combined organic layers were dried over MgSO<sub>4</sub>, filtered, and concentrated in vacuo. The crude mixture was purified by column chromatography on silica gel (petroleum: EA = 10:1~5:1) to afford the desired intermediate **30a**.

Following the Step 2 and Step 3 of the general procedure (4.2.3) used for the preparation of **7–19**, the desired products **30–39** were obtained using substituted bromobenzene (1.0 eq) and intermediate **30a** (1.2 eq) as the starting materials.

#### 4.2.5.1

2-(6-(2,2-Difluorobenzo[d][1,3]dioxol-5-yl)-1-((3-(trifluoromethyl)phenyl)sulfonyl)indolin-2-yl)acetic acid (**30**). Yield: 85%, white solid, purity: 97%. <sup>1</sup>H NMR (400 MHz, CDCl<sub>3</sub>) δ (ppm) 7.96 (s, 1H), 7.90 (d, *J* = 7.6 Hz, 1H), 7.82 (d, *J* = 7.2 Hz, 2H), 7.59 (t, *J* = 7.4 Hz, 1H), 7.29 (d, *J* = 9.0 Hz, 2H), 7.22 (d, *J* = 7.5 Hz, 1H), 7.15 (d, *J* = 4.2 Hz, 2H), 4.68 – 4.61 (m, 1H), 3.18 (d, *J* = 16.7 Hz, 1H), 3.00 (dd, *J* = 16.6, 9.4 Hz, 1H), 2.81 – 2.70 (m, 2H); <sup>13</sup>C NMR (150 MHz, CDCl<sub>3</sub>) δ (ppm) 175.3, 144.3, 143.4, 141.2, 140.6, 138.7, 137.0, 133.4, 131.9, 131.7 (d, *J* = 2.7 Hz), 130.4, 130.1, 130.0, 125.9, 124.5, 124.2 (d, *J* = 2.7 Hz), 123.8, 122.6, 122.0, 115.6, 109.7, 108.5, 59.2, 41.1, 34.5; MS (ESI) *m/z* 542.1 [M + H]<sup>+</sup>.

4.2.5.2 2-(6-(Benzof[d][1,3]dioxol-5-yl)-1-((3-(trifluoromethyl)phenyl)sulfonyl)indolin-2-yl)acetic acid (**31**). Yield: 82%, white solid, purity: 95%. <sup>1</sup>H NMR (400 MHz, CDCl<sub>3</sub>) δ (ppm) 7.97 (s, 1H), 7.89 (d, *J* = 7.7 Hz, 1H), 7.83 (s, 1H), 7.80 (d, *J* = 7.6 Hz, 1H), 7.57 (t, *J* = 7.8 Hz, 1H), 7.22 (d, *J* = 7.8 Hz, 1H), 7.08 (dd, *J* = 8.9, 7.8 Hz, 3H), 6.90 (d, *J* = 8.4 Hz, 1H), 6.02 (s, 2H), 4.64 (t, *J* = 9.4 Hz, 1H), 3.16 (dd, *J* = 16.6, 3.6 Hz, 1H), 2.97 (dd, *J* = 16.5, 9.3 Hz, 1H), 2.77 (dd, *J* = 16.5, 10.0 Hz, 1H), 2.69 (d, *J* = 17.0 Hz, 1H); <sup>13</sup>C NMR (150 MHz, CDCl<sub>3</sub>) δ (ppm) 174.7, 148.2, 147.4, 141.6, 140.9, 138.7, 134.8, 131.8 (d, *J* = 33.4 Hz), 130.1, 130.0, 129.9, 129.8 (d, *J* = 1.7 Hz), 129.6, 125.7, 124.2 (d, *J* = 3.3 Hz), 124.2, 120.8, 115.5, 108.6, 107.7, 101.3, 59.2, 41.0, 34.4; MS (ESI) *m/z* 506.1 [M + H]<sup>+</sup>.

#### 4.2.5.3

*2-(6-(2,3-Dihydrobenzofuran-5-yl)-1-((3-(trifluoromethyl)phenyl)sulfonyl)indolin-2-yl)acetic acid (32)*. Yield: 79%, white solid, purity: 96%. <sup>1</sup>H NMR (400 MHz, CDCl<sub>3</sub>) δ (ppm) 7.97 (d, *J* = 8.6 Hz, 1H), 7.86 (dd, *J* = 22.4, 8.4 Hz, 2H), 7.79 (t, *J* = 8.2 Hz, 1H), 7.56 (q, *J* = 8.2 Hz, 1H), 7.43 (d, *J* = 8.3 Hz, 1H), 7.34 (t, *J* = 8.4 Hz, 1H), 7.23 (d, *J* = 9.2 Hz, 1H), 7.08 (t, *J* = 8.3 Hz, 1H), 6.86 (t, *J* = 8.7 Hz, 1H), 4.63 (q, *J* = 8.8 Hz, 3H), 3.29 (q, *J* = 8.6 Hz, 2H), 3.20 – 3.12 (m, 1H), 3.00 – 2.92 (m, 1H), 2.81 – 2.64 (m, 2H); <sup>13</sup>C NMR (150 MHz, CDCl<sub>3</sub>) δ (ppm) 162.0, 142.2, 141.3, 138.5, 133.2, 129.8 (d, *J* = 39.0 Hz), 130.1, 130.0, 129.9, 129.8 (d, *J* = 2.5 Hz), 129.7, 129.1, 127.8, 127.1, 125.6, 124.2 (d, *J* = 10.1 Hz), 123.8, 115.3, 109.5, 71.6, 59.3, 40.9, 34.4, 31.9; MS (ESI) *m/z* 504.1 [M + H]<sup>+</sup>.

*4.2.5.4 2-(6-(3,5-Difluorophenyl)-1-((3-(trifluoromethyl)phenyl)sulfonyl)indolin-2-yl)acetic acid (33)*. Yield: 77%, pale yellow solid, purity: 94%. <sup>1</sup>H NMR (400 MHz, CDCl<sub>3</sub>) δ (ppm) 7.96 (s, 1H), 7.89 (d, *J* = 7.8 Hz, 1H), 7.85 (s, 1H), 7.82 (d, *J* = 7.6 Hz, 1H), 7.59 (t, *J* = 7.9 Hz, 1H), 7.32 – 7.28 (m, 1H), 7.15 (d, *J* = 7.9 Hz, 1H), 7.11 (d, *J* = 7.1 Hz, 2H), 6.83 (t, *J* = 8.7 Hz, 1H), 4.65 (t, *J* = 8.9 Hz, 1H), 3.17 (dd, *J* = 16.5, 3.9 Hz, 1H), 3.01 (dd, *J* = 16.8, 9.3 Hz, 1H), 2.81 – 2.70 (m, 2H); <sup>13</sup>C NMR (150 MHz, CDCl<sub>3</sub>) δ (ppm) 174.5, 164.2 (d, *J* = 13.5 Hz), 162.5 (d, *J* = 13.3 Hz), 143.7 (d, *J* = 13.3 Hz), 141.3, 139.6, 138.6, 131.8 (d, *J* = 13.3 Hz), 131.2, 130.1, 129.9, 127.6 (d, *J* = 48.0 Hz), 126.0, 124.4, 124.2 (d, *J* = 3.4 Hz), 123.8, 122.0, 115.5, 110.1 (dd, *J* = 20.6, 5.1 Hz), 102.9 (t, *J* = 25.3 Hz), 59.2, 40.9, 34.5; MS (ESI) *m/z* 498.1 [M + H]<sup>+</sup>.

*4.2.5.5 2-(6-(3-Chloro-5-fluorophenyl)-1-((3-(trifluoromethyl)phenyl)sulfonyl)indolin-2-yl)acetic acid (34)*. Yield: 73%, pale yellow solid, purity: 97%. <sup>1</sup>H NMR (400 MHz, CDCl<sub>3</sub>) δ (ppm) 7.97 (s, 1H), 7.89 (d, *J* = 7.9 Hz, 1H), 7.85 (s, 1H), 7.82 (d, *J* = 8.0 Hz, 1H), 7.59 (t, *J* = 7.8 Hz, 1H), 7.37 (s, 1H), 7.24 (s, 1H), 7.19 (d, *J* = 9.7 Hz, 1H), 7.15 (d, *J* = 8.0 Hz, 1H), 7.11 (d, *J* = 8.1 Hz, 1H), 4.65 (t, *J* = 9.2 Hz, 1H), 3.17 (dd, *J* = 16.7, 3.8 Hz, 1H), 3.01 (dd, *J* = 16.6, 9.3 Hz, 1H), 2.81 – 2.71 (m, 2H); <sup>13</sup>C NMR (150 MHz, CDCl<sub>3</sub>) δ (ppm) 175.1, 163.0 (d, *J* = 249.6 Hz), 143.7 (d, *J* = 8.6 Hz), 141.3, 139.4, 138.6, 135.5 (d, *J* = 10.9 Hz), 131.9 (d, *J* = 33.5 Hz), 131.3, 130.1 (d, *J* = 4.1 Hz), 128.9, 127.2, 126.0, 124.5, 124.2 (d, *J* = 2.9 Hz), 123.3, 122.0, 115.5, 115.3 (d, *J* = 24.9 Hz), 112.7 (d, *J* = 22.2 Hz), 59.2, 41.0, 34.5; MS (ESI) *m/z* 514.1 [M + H]<sup>+</sup>.

## 4.2.5.6

2-(6-(3-Fluoro-5-(trifluoromethyl)phenyl)-1-((3-(trifluoromethyl)phenyl)sulfonyl)indolin-2-yl)acetic acid (**35**). Yield: 78%, pale yellow solid, purity: 96%.  $^1\text{H}$  NMR (400 MHz,  $\text{CDCl}_3$ )  $\delta$  (ppm) 7.97 (s, 1H), 7.90 (d,  $J = 7.6$  Hz, 1H), 7.87 (s, 1H), 7.82 (d,  $J = 7.5$  Hz, 1H), 7.60 (d,  $J = 12.2$  Hz, 2H), 7.47 (d,  $J = 9.2$  Hz, 1H), 7.34 (d,  $J = 8.0$  Hz, 1H), 7.29 (d,  $J = 6.9$  Hz, 1H), 7.18 (d,  $J = 7.7$  Hz, 1H), 4.66 (t,  $J = 9.6$  Hz, 1H), 3.18 (dd,  $J = 16.7, 3.6$  Hz, 1H), 3.03 (dd,  $J = 16.9, 9.5$  Hz, 1H), 2.82 – 2.69 (m, 2H);  $^{13}\text{C}$  NMR (150 MHz,  $\text{CDCl}_3$ )  $\delta$  (ppm) 175.0, 162.8 (d,  $J = 247.8$  Hz), 143.8 (d,  $J = 7.3$  Hz), 141.4, 139.2, 138.6, 133.1 (d,  $J = 26.4$  Hz), 131.9 (d,  $J = 33.6$  Hz), 131.5, 130.1, 130.1, 129.9, 126.1, 124.6, 124.2, 123.8, 122.2 (d,  $J = 52.6$  Hz), 119.8, 117.6 (d,  $J = 21.8$  Hz), 115.57, 111.9 (d,  $J = 24.3$  Hz), 59.2, 41.0, 34.5; MS (ESI)  $m/z$  548.1  $[\text{M} + \text{H}]^+$ .

## 4.2.5.7

2-(6-(3-Fluoro-5-methoxyphenyl)-1-((3-(trifluoromethyl)phenyl)sulfonyl)indolin-2-yl)acetic acid (**36**). Yield: 77%, white solid, purity: 95%.  $^1\text{H}$  NMR (400 MHz,  $\text{CDCl}_3$ )  $\delta$  (ppm) 7.97 (s, 1H), 7.89 (d,  $J = 8.0$  Hz, 1H), 7.87 (s, 1H), 7.81 (d,  $J = 7.8$  Hz, 1H), 7.58 (t,  $J = 7.8$  Hz, 1H), 7.28 (s, 1H), 7.13 (d,  $J = 7.8$  Hz, 1H), 6.89 (d,  $J = 12.9$  Hz, 2H), 6.64 (d,  $J = 10.5$  Hz, 1H), 4.65 (t,  $J = 9.5$  Hz, 1H), 3.87 (s, 3H), 3.17 (dd,  $J = 16.7, 3.8$  Hz, 1H), 3.00 (dd,  $J = 16.8, 9.4$  Hz, 1H), 2.78 (dd,  $J = 16.7, 10.1$  Hz, 1H), 2.71 (d,  $J = 17.0$  Hz, 1H);  $^{13}\text{C}$  NMR (150 MHz,  $\text{CDCl}_3$ )  $\delta$  (ppm) 175.5, 163.9 (d,  $J = 245.0$  Hz), 161.2 (d,  $J = 11.6$  Hz), 143.1 (d,  $J = 9.7$  Hz), 141.0, 140.8, 138.7, 131.9 (q,  $J = 66.0$  Hz), 130.7, 130.1 (d,  $J = 9.0$  Hz), 130.0, 125.8, 124.5, 124.2, 123.8, 122.0, 115.6, 109.0, 106.5 (d,  $J = 22.7$  Hz), 100.6 (d,  $J = 25.1$  Hz), 59.2, 55.7, 41.1, 34.5; MS (ESI)  $m/z$  510.1  $[\text{M} + \text{H}]^+$ .

4.2.5.8 2-(6-(3-Ethoxy-5-fluorophenyl)-1-((3-(trifluoromethyl)phenyl)sulfonyl)indolin-2-yl)acetic acid (**37**).

Yield: 72%, white solid, purity: 97%.  $^1\text{H}$  NMR (400 MHz,  $\text{DMSO}-d_6$ )  $\delta$  (ppm) 8.09 (dd,  $J = 18.3, 7.1$  Hz, 2H), 7.92 (s, 1H), 7.81 (t,  $J = 7.4$  Hz, 1H), 7.65 (s, 1H), 7.37 (d,  $J = 7.5$  Hz, 1H), 7.24 (d,  $J = 7.1$  Hz, 1H), 6.98 (d,  $J = 9.9$  Hz, 1H), 6.94 (s, 1H), 6.85 (d,  $J = 10.0$  Hz, 1H), 4.71 (t,  $J = 6.9$  Hz, 1H), 4.12 (q,  $J = 6.0$  Hz, 2H), 3.00 – 2.93 (m, 1H), 2.80 (t,  $J = 14.7$  Hz, 2H), 2.71 – 2.65 (m, 1H), 1.36 (t,  $J = 6.0$  Hz, 3H);  $^{13}\text{C}$  NMR (150 MHz,  $\text{DMSO}-d_6$ )  $\delta$  (ppm) 171.3, 163.2 (d,  $J =$

242.6 Hz), 160.2 (d,  $J = 12.1$  Hz), 142.6 (d,  $J = 10.3$  Hz), 140.6, 138.8, 137.6, 131.9, 131.3, 130.8, 130.4, 129.6 (d,  $J = 21.9$  Hz), 126.1, 124.0, 123.3 (d,  $J = 2.5$  Hz), 122.0, 114.0, 109.1, 105.3 (d,  $J = 22.7$  Hz), 100.8 (d,  $J = 25.0$  Hz), 63.6, 59.5, 41.1, 33.7, 14.3; MS (ESI)  $m/z$  524.1  $[M + H]^+$ .

#### 4.2.5.9

*2-(6-(3-Fluoro-5-isopropoxyphenyl)-1-((3-(trifluoromethyl)phenyl)sulfonyl)indolin-2-yl)acetic acid (38)*. Yield: 70%, white solid, purity: 98%.  $^1\text{H}$  NMR (400 MHz,  $\text{DMSO-}d_6$ )  $\delta$  (ppm) 7.94 (s, 1H), 7.87 (d,  $J = 7.9$  Hz, 1H), 7.83 (s, 1H), 7.78 (d,  $J = 7.7$  Hz, 1H), 7.55 (t,  $J = 7.8$  Hz, 1H), 7.23 (d,  $J = 7.7$  Hz, 1H), 7.09 (d,  $J = 7.8$  Hz, 1H), 6.88 (s, 1H), 6.83 (d,  $J = 9.3$  Hz, 1H), 6.59 (d,  $J = 10.7$  Hz, 1H), 4.66 – 4.55 (m, 2H), 3.08 (dd,  $J = 16.5, 3.6$  Hz, 1H), 2.95 (dd,  $J = 16.8, 9.2$  Hz, 1H), 2.69 (dd,  $J = 13.4, 6.7$  Hz, 2H), 1.37 (s, 3H), 1.36 (s, 3H);  $^{13}\text{C}$  NMR (150 MHz,  $\text{DMSO-}d_6$ )  $\delta$  (ppm) 172.9, 163.8 (d,  $J = 244.5$  Hz), 159.4 (d,  $J = 11.5$  Hz), 143.1 (d,  $J = 9.9$  Hz), 141.1, 140.6, 138.8, 131.9 (q,  $J = 67.5$  Hz), 131.0, 130.0 (d,  $J = 20.2$  Hz), 129.8 (d,  $J = 2.7$  Hz), 125.7, 124.3, 124.1 (d,  $J = 3.2$  Hz), 123.8, 122.0, 115.6, 110.8, 106.2 (d,  $J = 22.6$  Hz), 102.0 (d,  $J = 24.8$  Hz), 70.5, 59.5, 41.2, 34.4, 21.9 (d,  $J = 4.8$  Hz); MS (ESI)  $m/z$  538.1  $[M + H]^+$ .

#### 4.2.5.10

*2-(6-(3-(Trifluoromethoxy)phenyl)-1-((3-(trifluoromethyl)phenyl)sulfonyl)indolin-2-yl)acetic acid (39)*. Yield: 76%, white solid, purity: 96%.  $^1\text{H}$  NMR (400 MHz,  $\text{CDCl}_3$ )  $\delta$  (ppm) 7.96 (s, 1H), 7.91 (d,  $J = 7.8$  Hz, 1H), 7.87 (s, 1H), 7.80 (d,  $J = 7.4$  Hz, 1H), 7.58 (t,  $J = 7.8$  Hz, 1H), 7.50 (dd,  $J = 20.0, 7.5$  Hz, 2H), 7.42 (s, 1H), 7.31 – 7.23 (m, 2H), 7.15 (d,  $J = 7.7$  Hz, 1H), 4.69 – 4.67 (m, 1H), 3.16 (d,  $J = 16.0$  Hz, 1H), 3.00 (dd,  $J = 16.6, 9.2$  Hz, 1H), 2.76 (dd,  $J = 27.6, 13.3$  Hz, 2H);  $^{13}\text{C}$  NMR (150 MHz,  $\text{CDCl}_3$ )  $\delta$  (ppm) 175.4, 149.7, 142.6, 141.2, 140.3, 138.7, 131.8 (d,  $J = 33.5$  Hz), 130.9, 130.1 (d,  $J = 6.3$  Hz), 130.0, 129.9, 128.9, 127.2, 125.9, 125.6, 124.6, 124.2 (d,  $J = 2.4$  Hz), 121.7 (d,  $J = 98.1$  Hz), 119.9, 119.8, 115.7, 59.4, 41.3, 34.5; MS (ESI)  $m/z$  546.1  $[M + H]^+$ .

### 4.3 Biological Assays

#### 4.3.1 ROR $\gamma$ Dual FRET Assay

The assay was performed in an assay buffer consisting of 50 mM NaF, 50 mM

3-(*N*-morpholino)propanesulfonic acid (pH 7.4), 0.05 mM 3-[(3-cholamidopropyl)dimethylammonio]propanesulfonate, 0.1 mg/mL bovine serum albumin, and 10 mM dithiothreitol in 384-well plates. The total volume was 25  $\mu$ L/well. The europium-labeled SRC1 solution was prepared by adding an appropriate amount of biotinylated SRC and europium labeled streptavidin into assay buffer, with final concentrations of 20 and 10 nM, respectively. The allophycocyanin (APC)-labeled-LBD solution was prepared by adding an appropriate amount of biotinylated RORc-LBD and APC-labeled streptavidin at final concentrations of 20 and 10 nM, respectively. After 15 mins of incubation at room temperature, a 20-fold excess of biotin was added and incubated for 10 mins at room temperature to block the remaining free streptavidin. Equal volumes of europium-labeled SRC and APC-labeled RORc-LBD were dispensed into 384-well assay plates at 25  $\mu$ L volume/well. The 384-well assay plates had 100 nL of test compound in DMSO predisposed into each well. The plates were incubated for 1 h at room temperature and then read on Envision in LANCE mode configured for europium-APC labels.

#### 4.3.2 ROR $\gamma$ GAL4 Reporter Gene Assay

hROR $\gamma$  LBD coding sequence was inserted into a pBIND expression vector (Promega, E1581) to express ROR-GAL4 binding domain chimeric receptors. This expression vector and a reporter vector (pGL4.35 which carries a stably integrated GAL4 promoter driven luciferase reporter gene [luc2P/9XGAL4 UAS/Hygro]) were co-transfected into HEK293T host cells. Upon agonist binding to the corresponding ROR-GAL4 chimeric receptor, the chimeric receptor binds to the GAL4 binding sites and stimulates the reporter gene. In the presence of inverse agonist, agonist will bind competitively to the nuclear receptor and activate the reporter gene transcription. HEK293T cells were cultured in a culture medium composed of DMEM containing 5% charcoal-treated FBS at 37 °C under 5% CO<sub>2</sub> atmosphere, as ATCC recommended. Before assay, the cells were washed with PBS to remove phenol red and suspended in phenol red-free medium (phenol red-free DMEM containing 5% charcoal-treated FBS and Penicillin-Streptomycin (10000 U/mL) to a proper concentration.  $6 \times 10^6$  HEK293T cells were seeded into a 100 mm dish and incubated for 16 h. To a reagent mixture of Trans-IT reagent and Opti-MEM (Invitrogen) was added plasmid DNA (used as 0.5 mg/mL stocks), containing 5  $\mu$ g ROR $\gamma$  plasmid and 5  $\mu$ g pGL4.35 luciferase plasmid. The mixture was added

to the cells in the 100 mm dish and incubated for 5-6 h. Test compounds were serially diluted in DMSO to 5-6 doses. LYC-55716 was used as the positive control and 100% DMSO was used as vehicle control. Compounds (25 nL) were transferred into a 384-well plate (white opaque) using Echo550. Then seeded the cells at 15,000 cells/well into the 384-well plate using phenol red-free DMEM containing 5% charcoal-treated FBS and 0.25  $\mu$ M ursolic acid. Cells were incubated for 16–20 h at 37 °C under 5% CO<sub>2</sub> atmosphere. 25  $\mu$ L of Steady-Glo™ Luciferase Assay Reagent was added into each well of the 384-well plate. Shake the plate (avoiding light) for 5 mins on a plate shaker. Record the luminescence value on Envision 2104 plate reader. EC<sub>50</sub> values were determined by the nonlinear regression analysis of dose-response curves.

#### 4.4 Aqueous Solubility Determination

Compounds **1-3**, **14** were dissolved in DMSO to a concentration of 10 mM as the stock solutions. These solutions were diluted into PBS buffer (pH 7.46, 100 mM, with 3.3 mM MgCl<sub>2</sub>) to a final compound concentration of 100  $\mu$ M. The samples were incubated at 37 °C in water bath for 120 mins, followed by filtration. The filtrates were then diluted with 70% ACN as needed. To the dilutions was added an internal standard solution meanwhile as stop solution. LC-MS/MS was used to determine compound concentrations in the prepared samples. Ketoconazole and nicardipine were tested as the control with solubility of 31.1  $\mu$ M and 5.01  $\mu$ M, respectively.

#### 4.5 Microsomal Stability Assay

Mouse liver microsomes (0.5 mg/mL), PBS and NADPH cofactors were added to the incubation system. The system was pre-incubated for 10 mins at 37 °C, and then test compounds were added to start the reaction at a final concentration of 1  $\mu$ M. The reaction was then evaluated at 0, 5, 10, 20, 30 and 60 mins and was terminated by the addition of acetonitrile. Samples were centrifuged for 20 mins at 4000 rpm at 4 °C, and the supernatant was analysed using HPLC-MS/MS. Percentage of the parent remaining was calculated considering the percent parent area at 0 min as 100%, and the peak areas at other time points are converted into corresponding residual amounts according to the control.  $t_{1/2}$  and CL<sub>int (mic)</sub> were calculated by equations as follow:

$$C_t = C_0 \cdot e^{-k_e \cdot t}$$

$$\text{when } C_t = \frac{1}{2} C_0,$$

$$T_{1/2} = \frac{\ln 2}{k_e} = \frac{0.693}{k_e}$$

$$CL_{\text{int(mic)}} = \frac{0.693}{\text{In vitro } T_{1/2}} \cdot \frac{1}{\text{mg / mL microsomal protein in reaction system}}$$

$$CL_{\text{int(liver)}} = CL_{\text{int(mic)}} \cdot \frac{\text{mg microsomes}}{\text{g liver}} \cdot \frac{\text{g liver}}{\text{kg body weight}}$$

#### 4.6 Mouse PK Study

Male CD-1 mice were intravenously or orally administered a single dose of the test compound **14** at 1 mg/kg (5%DMSO, 40%PEG400, 55%(20% $\beta$ -CD) solution) or 5 mg/kg (suspension in 1%DMSO, 99%(1% methylcellulose)), respectively. After the administration, blood samples were collected over a 24 h time course and centrifuged to obtain the plasma. The resulting plasma samples were precipitated with acetonitrile and injected to LC-MS/MS system for compound analysis. PK parameters were calculated from plasma concentration–time curves using noncompartmental analysis.

#### 4.7 Molecular Docking Studies

Molecular docking was carried out using Schrodinger 3.5 software package. The co-crystal structure of ROR $\gamma$ t LBD (PDB: 4NIE) was selected and processed using the Protein Preparation Wizard including water deletion, addition of missing hydrogen atoms as well as adjustment of the tautomerization and protonation states of histidine. The compound 3D structures were subjected to energy minimization with force field (OPLS\_2005) before submitting to the docking procedure. The docking grid was centered according to the ligand position, and the bounding box was set to 15 Å. This docking was performed with Glide-docking using Extra Precision (GlideXP) algorithm. The final ranking from the docking was based on the docking score, which combines the Epik state penalty with the Glide Score. High-scoring complexes were inspected visually to select the most reasonable solution.

#### Acknowledgements

This work was supported by National Science Foundation of China (Grant Numbers: 81573276; 81874287), Shanghai Bio-pharmaceutical Science and Technology Supporting Plan (Grant Number: 17431902100; 19431900100), National Science and Technology Major Project (Grant Number: 2018ZX09711002-003-014), and Fudan-SIMM Joint Research Fund (Grant Number: FU-SIMM20174007).

#### References

- [1] I.I. Ivanov, B.S. McKenzie, L. Zhou, C.E. Tadokoro, A. Lepelley, J.J. Lafaille, D.J. Cua, D.R. Littman, The orphan nuclear receptor ROR $\gamma$ t directs the differentiation program of proinflammatory IL-17+ T helper cells, *Cell* 126 (2006) 1121-1133.
- [2] C. Lock, G. Hermans, R. Pedotti, A. Brendolan, E. Schadt, H. Garren, A. Langer-Gould, S. Strober, B. Cannella, J. Allard, P. Klonowski, A. Austin, N. Lad, N. Kaminski, S.J. Galli, J.R. Oksenberg, C.S. Raine, R. Heller, L. Steinman, Gene-microarray analysis of multiple sclerosis lesions yields new targets validated in autoimmune encephalomyelitis, *Nat. Med.* 8 (2002) 500-508.
- [3] L.A. Tesmer, S.K. Lundy, S. Sarkar, D.A. Fox, Th17 cells in human disease, *Immunol. Rev.* 223 (2008) 87-113.
- [4] V.B. Pandya, S. Kumar, Sachchidanand, R. Sharma, R.C. Desai, Combating autoimmune diseases with retinoic acid receptor-related orphan receptor- $\gamma$  (ROR $\gamma$  or RORc) inhibitors: Hits and misses, *J. Med. Chem.* 61 (2018) 10976-10995.
- [5] a. F. Narjes, Y. Xue, S. von Berg, J. Malmberg, A. Llinas, R.I. Olsson, J. Jirholt, H. Grindebacke, A. Leffler, N. Hossain, M. Lepistö, L. Thunberg, H. Leek, A. Aagaard, J. McPheat, E.L. Hansson, E. Bäck, S. Tångefjord, R. Chen, Y. Xiong, G. Hongbin, T.G. Hansson, Potent and orally bioavailable inverse agonists of ROR $\gamma$ t resulting from structure-based design, *J. Med. Chem.* 61 (2018) 7796-7813; b. M.E. Schnute, M. Wennerstål, J. Alley, M. Bengtsson, J.R. Blinn, C.W. Bolten, T. Braden, T. Bonn, B. Carlsson, N. Caspers, M. Chen, C. Choi, L.P. Collis, K. Crouse, M. Färnegårdh, K.F. Fennell, S. Fish, A.C. Flick, A. Goos-Nilsson, H. Gullberg, P.K. Harris, S.E. Heasley, M. Hegen, A.E. Hromockyj, X. Hu, B. Husman, T. Janosik, P. Jones, N. Kaila, E. Kallin, B. Kauppi, J.R. Kiefer, J. Knafels, K. Koehler, L. Kruger, R.G. Kurumbail, R.E. Kyne, W. Li, J. Löfstedt, S.A. Long, C.A. Menard, S. Mente, D. Messing, M.J. Meyers, L. Napierata, D. Nöteberg, P. Nuhant, M.J. Pelc, M.J. Prinsen, P. Rhönnstad, E. Backström-Rydin, J. Sandberg, M. Sandström, F. Shah, M. Sjöberg, A. Sundell, A.P. Taylor, A. Thorarensen, J.I. Trujillo, J.D. Trzuppek, R. Unwalla, F.F. Vajdos, R.A. Weinberg, D. C. Wood, L. Xing, E. Zamaratski, C.W. Zapf, Y. Zhao, A. Wilhelmsson, G. Berstein, Discovery of 3-Cyano-N-(3-(1-isobutyrylpiperidin-4-yl)-1-methyl-4-(trifluoromethyl)-1H-pyrrolo[2,3-b]pyridin-5-yl)benzamide: A potent, selective, and orally bioavailable retinoic acid receptor-related orphan receptor C2 inverse agonist, *J. Med. Chem.* 61 (2018) 10415-10439; c. D.A. Carcache, A. Vulpetti, J. Kallen, H. Mattes, D. Orain, R. Stringer, E. Vangrevelinghe, R.M. Wolf, K. Kaupmann, J. Ottl, J. Dawson, N.G. Cooke, K. Hoegenauer, A. Billich, J. Wagner, C. Guntermann, S. Hintermann, Optimizing a weakly binding fragment into a potent ROR $\gamma$ t inverse agonist with efficacy in an in vivo inflammation model, *J. Med. Chem.* 61 (2018) 6724-6735.
- [6] Y. Zhang, X. Wu, X. Xue, C. Li, J. Wang, R. Wang, C. Zhang, C. Wang, Y. Shi, L. Zou, Q. Li, Z. Huang, X. Hao, K. Loomes, D. Wu, H.-W. Chen, J. Xu, Y. Xu, Discovery and characterization of XY101, a potent, selective, and orally bioavailable ROR $\gamma$  inverse agonist for treatment of castration-resistant prostate cancer, *J. Med. Chem.* 62 (2019) 4716-4730.
- [7] J. Wang, J.X. Zou, X. Xue, D. Cai, Y. Zhang, Z. Duan, Q. Xiang, J.C. Yang, M.C. Louie, A.D. Borowsky, A.C. Gao, C.P. Evans, K.S. Lam, J. Xu, H.-J. Kung, R.M. Evans, Y. Xu, H.-W. Chen, ROR $\gamma$  drives androgen receptor expression and represents a therapeutic target in castration-resistant prostate cancer, *Nat. Med.* 22(2016) 488-496.
- [8] I. Kryczek, S. Wei, L. Vatan, J. Escara-Wilke, W. Szeliga, E.T. Keller, W. Zou, Cutting edge: opposite effects of IL-1 and IL-2 on the regulation of IL-17+ T cell pool IL-1 subverts

- IL-2-mediated suppression, *J. Immunol.* 179 (2007) 1423-1426.
- [9] I. Kryczek, M. Banerjee, P. Cheng, L. Vatan, W. Szeliga, S. Wei, E. Huang, E. Finlayson, D. Simeone, T.H. Welling, A. Chang, G. Coukos, R. Liu, W. Zou, Phenotype, distribution, generation, and functional and clinical relevance of Th17 cells in the human tumor environments, *Blood* 114 (2009) 1141-1149.
- [10] N. Martin-Orozco, P. Muranski, Y. Chung, X.O. Yang, T. Yamazaki, S. Lu, P. Hwu, N.P. Restifo, W.W. Overwijk, C. Dong, T helper 17 cells promote cytotoxic T cell activation in tumor immunity, *Immunity* 31 (2009) 787-798.
- [11] X. Hu, X. Liu, J. Moisan, Y. Wang, C.A. Lesch, C. Spooner, R.W. Morgan, E.M. Zawidzka, D. Mertz, D. Bousley, K. Majchrzak, I. Kryczek, C. Taylor, C. Van Huis, D. Skalitzky, A. Hurd, T.D. Aicher, P.L. Toogood, G.D. Glick, C.M. Paulos, W. Zou, L.L. Carter, Synthetic ROR $\gamma$  agonists regulate multiple pathways to enhance antitumor immunity, *OncoImmunology* 5 (2016) e1254854.
- [12] M.R. Chang, V. Dharmarajan, C. Doebelin, R.D. Garcia-Ordonez, S.J. Novick, D.S. Kuruvilla, T.M. Kamenecka, P.R. Griffin, Synthetic ROR $\gamma$ t agonists enhance protective immunity, *ACS Chem. Biol.* 11 (2016) 1012-1018.
- [13] R. Qiu, Y. Wang, Retinoic acid receptor-related orphan receptor  $\gamma$ t (ROR $\gamma$ t) agonists as potential small molecule therapeutics for cancer immunotherapy, *J. Med. Chem.* 61 (2018) 5794-5804.
- [14] Y. Wang, N. Kumar, P. Nuhant, M.D. Cameron, M.A. Istrate, W.R. Roush, P.R. Griffin, T.P. Burris, Identification of SR1078, a synthetic agonist for the orphan nuclear receptors ROR $\alpha$  and ROR $\gamma$ , *ACS Chem. Biol.* 5 (2010) 1029-1034.
- [15] R.I. Olsson, Y. Xue, S. von Berg, A. Aagaard, J. McPheat, E.L. Hansson, J. Bernström, P. Hansson, J. Jirholt, H. Grindebacke, A. Leffler, R. Chen, Y. Xiong, H. Ge, T.G. Hansson, F. Narjes, Benzoxazepines achieve potent suppression of IL-17 release in human T-helper 17 (Th17) cells through an induced-fit binding mode to the nuclear receptor ROR $\gamma$ , *ChemMedChem* 11 (2016) 207-216.
- [16] D.J. Marcotte, Y. Liu, K. Little, J.H. Jones, N.A. Powell, C.P. Wildes, L.F. Silvian, J.V. Chodaparambil, Structural determinant for inducing ROR $\gamma$  specific inverse agonism triggered by a synthetic benzoxazinone ligand, *BMC Structural Biology* 16 (2016) 1-9.
- [17] T. Yukawa, Y. Nara, M. Kono, A. Sato, T. Oda, T. Takagi, T. Sato, Y. Banno, N. Taya, T. Imada, Z. Shiokawa, N. Negoro, T. Kawamoto, R. Koyama, N. Uchiyama, R. Skene, I. Hoffman, C.H. Chen, B. Sang, G. Snell, R. Katsuyama, S. Yamamoto, J. Shirai, Design, synthesis, and biological evaluation of retinoic acid-related orphan receptor  $\gamma$ t (ROR $\gamma$ t) agonist structure-based functionality switching approach from in house ROR $\gamma$ t inverse agonist to ROR $\gamma$ t agonist, *J. Med. Chem.* 62 (2019) 1167-1179.
- [18] O. Rene, B.P. Fauber, L. Boenig Gde, B. Burton, C. Eidenschenk, C. Everett, A. Gobbi, S.G. Hymowitz, A.R. Johnson, J.R. Kiefer, M. Liimatta, P. Lockey, M. Norman, W. Ouyang, H.A. Wallweber, H. Wong, Minor structural change to tertiary sulfonamide ROR $\gamma$ c ligands led to opposite mechanisms of action, *ACS Med. Chem. Lett.* 6 (2015) 276-281.
- [19] T. Yang, Q. Liu, Y. Cheng, W. Cai, Y. Ma, L. Yang, Q. Wu, L.A. Orband-Miller, L. Zhou, Z. Xiang, M. Huxdorf, W. Zhang, J. Zhang, J.N. Xiang, S. Leung, Y. Qiu, Z. Zhong, J.D. Elliott, X. Lin, Y. Wang, Discovery of tertiary amine and indole derivatives as potent ROR $\gamma$ t inverse agonists, *ACS Med. Chem. Lett.* 5 (2014) 65-68.
- [20] Y. Wang, T. Yang, Q. Liu, Y. Ma, L. Yang, L. Zhou, Z. Xiang, Z. Cheng, S. Lu, L.A.

- Orband-Miller, W. Zhang, Q. Wu, K. Zhang, Y. Li, J.N. Xiang, J.D. Elliott, S. Leung, F. Ren, X. Lin, Discovery of *N*-(4-aryl-5-aryloxy-thiazol-2-yl)-amides as potent ROR $\gamma$ t inverse agonists, *Bioorg. Med. Chem.* 23 (2015) 5293-5302.
- [21] Y. Wang, W. Cai, T. Tang, Q. Liu, T. Yang, L. Yang, Y. Ma, G. Zhang, Y. Huang, X. Song, L.A. Orband-Miller, Q. Wu, L. Zhou, Z. Xiang, J.N. Xiang, S. Leung, L. Shao, X. Lin, M. Lobera, F. Ren, From ROR $\gamma$ t agonist to two types of ROR $\gamma$ t inverse agonists, *ACS Med. Chem. Lett.* 9 (2018) 120-124.
- [22] C. Doebelin, R. Patouret, R.D. Garcia-Ordonez, M.R. Chang, V. Dharmarajan, D.S. Kuruvilla, S.J. Novick, L. Lin, M.D. Cameron, P.R. Griffin, T.M. Kamenecka, N-Arylsulfonyl indolines as retinoic acid receptor-related orphan receptor  $\gamma$  (ROR $\gamma$ ) agonists, *ChemMedChem* 11 (2016) 2607-2620.
- [23] G.D. Glick, P.L. Toogood, X. Hu, T.D. Aicher, L.L. Celester, X. Liu, C.B. Taylor, C.A. Vanhuis, Adoptive cellular therapy using an agonist of retinoic acid receptor-related orphan receptor gamma & related therapeutic methods, WO2015131035A1, 2015.
- [24] <https://clinicaltrials.gov/ct2/results?term=LYC-55716>.
- [25] T.D. Aicher, C.B. Taylor, C.A. Vanhuis, Aryl dihydro-2*H*-benzo[*b*][1,4]oxazine sulfonamide and related compounds for use as agonists of ROR $\gamma$  and the treatment of disease. WO2016201225A1, 2016.

### Research highlights

- A series of aryl-substituted indole and indoline derivatives was discovered as novel ROR $\gamma$ t agonists
- **14** showed good ROR $\gamma$ t agonism activity in both dual FRET assay and GAL-4 reporter gene assay
- **14** showed high metabolic stability, improved aqueous solubility and excellent mouse PK profile
- The binding mode of the most potent (*S*)-enantiomer of **14** in ROR $\gamma$ t ligand binding domain (LBD) was discussed